A membrane-driven biochemical oscillator tunable by the volume to surface area ratio

Jonathan Fischer, Ezra Greenberg, Yue Moon Ying, Samuel L. Foley, Margaret E. Johnson*

TC Jenkins Department of Biophysics, Johns Hopkins University, 3400 N Charles St, Baltimore, MD 21218.

**Corresponding Author*: margaret.johnson@jhu.edu ph: 410-516-2376

ABSTRACT

Protein based biochemical oscillators have garnered particular interest recently, due to their potential applications in synthetic biology and advantages over genetic oscillators. Here, we present a computational model introducing a novel biochemical oscillator that can be tuned by manipulating the volume to surface area ratio of the reaction system. Adapted from a reaction network using components of the endocytosis machinery, the model exploits membrane localization of lipid-modifying enzymes to produce periodicity in the concentrations of membrane bound species. The degree of membrane localization is linearly coupled to t he volume to surface area ratio of the reaction volume, enabling the chemical dynamics to be directly tuned through geometric manipulation without any need for engineering the underlying biochemistry. In some regimes, the system geometry can be used to tune the oscillation period, or the period can be used to sense the system geometry. Other reaction systems like self-assembly or bioluminescence can be easily coupled to the oscillator through an adaptor binding interface, opening a wide range of potential applications, like timed drug delivery or cell morphology sensors. Through computer simulation and mathematical analysis, our model informs future in-vivo application of membrane-localization oscillators (MLOs).

Commented [MJ1]: I like the abstract, the sentences are concise and informative. You do need at least one or two sentences prior to "Here we" to set up the field. It is rare to skip that, and so something about oscillations in biology makes the most sense.

INTRODUCTION

Biological oscillators perform the crucial role of synchronizing biological processes to each other and to external stimuli. The ability of biological oscillators to temporally coordinate reactions in noisy cellular environments makes them attractive elements for artificial biological circuits and other synthetic applications. While genetic oscillators such as the repressilator [1] have traditionally dominated engineered oscillator designs, recent interest has shifted towards post-translational protein oscillators (PTOs) due to their numerous engineering advantages [2]. PTOs can be driven by fast and reversible post-translational modifications such as phosphorylation, offering a wider range of timescales for them to operate in when compared to transcription-translation driven genetic oscillators [3]. Interesting work has already been done on this front, such as a recent model of a self-assembly-based post translational oscillator, but the toolbox of mechanisms available to engineer such dynamics remains limited [4].

The dynamical properties of PTOs aren't limited to strictly protein substrates, and functional equivalents to many PTO motifs can use lipid species instead to host modification states. Various lipid membranes found in nature already exhibit dynamic interconversion between different modification states, particularly through processes like phosphorylation and dephosphorylation. For instance, the plasma membrane contains phosphatidylinositols that cycle between mono-, bis-, and tris-phosphorylated states, regulated by kinases like PI3K and phosphatases such as PTEN. Similarly, sphingolipids in the Golgi apparatus undergo rapid interconversion between ceramide, sphingomyelin, and glycosphingolipids. These lipid modification pathways are often essential cell signaling mechanisms, and can be adapted as motifs for synthetic systems.

One biological system known to produce membrane oscillations is phosphoinositide (PIP) regulation in lipid membranes [5]. PIPs are membrane lipids important for selective membrane recruitment of proteins and can be phosphorylated or dephosphorylated by lipid-modifying enzymes into a variety of PIP species

Commented [MJ2]: Specific examples with references. This is a nice paragraph!

Commented [MJ3]: Not quite sure what you mean by this.

Commented [MJ4]: Again, good paragraph, needs more references.

Commented [JF5]: Need to find consistent way to use words like "system", "motif", "pathway"

Commented [MJ7R6]: I would not say "membrane oscillations" because I'm not sure what's oscillating. We can say temporal and spatial oscillations in proteins localized to the membrane, generating patterns.

[6]. By controlling the local composition of these PIP species in the lipid membrane, the cell can tune the membrane specificity for various protein complexes. As the enzymes controlling the phosphorylation state can themselves be membrane localized as a function of the lipid composition [7], there are nonlinear feedback mechanisms between enzymatic activity and PIP metabolism [8] that can drive oscillations.

Membrane localization can generate nonlinear feedback because it selectively accelerates reactions and assembly by transitioning the diffusional search for binding partners from 3D to 2D, known as dimensional reduction. Dimensional reduction can enhance binding speeds and probabilities in 2D vs 3D dependent on changes to diffusion times of species, changes in accessible configurations and free energy landscapes of bound vs unbound species, and (typically) increased reactant density in the lower dimensional space. The effective binding enhancement has been mathematically modeled in recent work by Osman et al as a function of the volume to surface area ratio (V/A) of the system, which scales the forward kinetics of biomolecular reactions [9]. Using a physiologically realistic range of cell V/A, the binding affinity between membrane-localized reactants can be enhanced by multiple orders of magnitude compared to their counterparts in 3D diffusive space, as can the timescales of dimerization[Cite Mishra et

Commented [EG8]: This is a little awkward. Maybe. "has been mathematically modeled in recent work by Osman et al as a linear scaling of the forward kinetics with the volume to surface area ration (V/A)." I think what you are talking about is just multiplying ka by DF which is why I said linear. Also, is it "biomolecular" here as written or "bimolecular" or can it just be "reactions" with no adjective?

al, 2021].

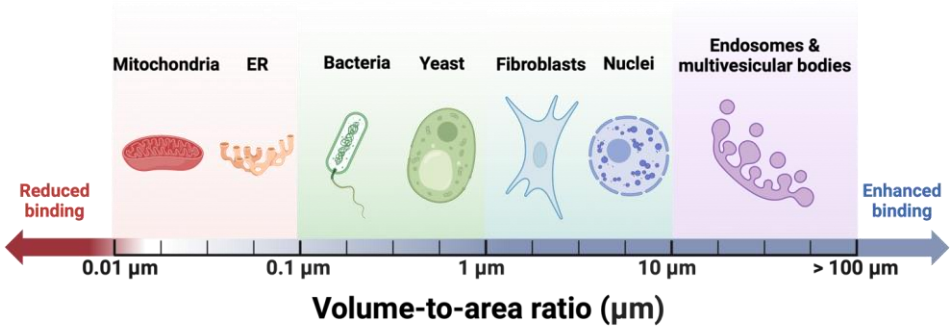

Importantly though, membrane localization is not a static binding enhancement; protein domains that bind the membrane directly target specific (typically phosphorylated) lipids, and thus changes to membrane composition alter localization propensities. The activity of the previously mentioned lipid-modifying enzymes, both kinases and phosphatases, can change the density of phosphorylated lipids on the membrane in space and time. As a result, by dynamically tuning the membrane lipid composition, cells have spatiotemporal control of specific membrane-protein affinities that can allow the encoding of complex molecular logic and spatiotemporal memory in the lipid membrane.

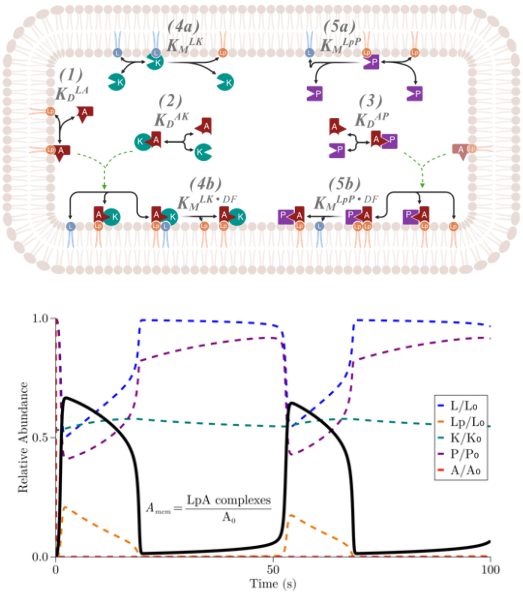

Figure 1: Schematic representation of the lipid-modifying enzymatic reaction network driving oscillatory dynamics.

(a) The model centers around the interconversion of phosphatidylinositol 4-phosphate (PIP, L) and phosphatidylinositol 4,5-bisphosphate (PIP2, Lp). The adaptor protein AP2 (A) binds to PIP2 (reaction 1), facilitating the recruitment of the kinase PIP5K (K) and the phosphatase synaptojanin (P) to the membrane through reactions 2 and 3, respectively. PIP5K binds to its ligand PIP (reaction 4a), while synaptojanin binds to its ligand PIP2 (reaction 5a). Reactions 4b and 5b represent the membrane-localized versions of these catalytic reactions, where PIP5K or synaptojanin is anchored to the membrane via the PIP2-AP2 complex. The dimensionality factor (DF) scales the reaction rates for reactions occurring in 2D on the membrane versus those in the 3D cytoplasm, representing the effect of membrane localization on reaction kinetics. Arrows depict the directionality of reactions, with red arrows indicating the primary forward reactions and gray arrows indicating reversible binding interactions.

However, to what extent membrane lipid composition can be exploited to drive stable oscillations has not explored previously. To bridge this gap, our study develops a minimal general model for a biochemical oscillator driven by membrane localization, offering insights into the coordination of reaction dynamics through geometric cues. Our inspiration and general reaction scheme was drawn from the PIP-mediated process of clathrin-mediated endocytosis (CME), where dynamically tuned membrane localization of

Commented [EG9]: Not sure that this statement is needed. "Geometric cues?"

endocytic machinery is necessary to control the expensive process of clathrin-coat assembly. In CME, the phosphorylated lipid PIP2 is effectively the “on” switch by which the cell signals recruitment of the endocytic machinery for cargo uptake. This recruitment signal is conveyed via the adaptor protein AP2, which has multiple PIP2 specific lipid binding interfaces and protein binding interfaces that indirectly localize the essential structural protein clathrin, which does not bind lipids, to the membrane. Like other biological switches, a positive feedback loop exists to discretize concentrations into binary logic: the kinase PIP5K accelerates its own activity through increasing the amount of PIP2 anchors, and the phosphatase synaptojanin utilizes to amplify its conversion of PIP2 back to PIP for the eventual “off” signal. Through the activity of lipid-modifying kinases and phosphatases, the amount of PIP2 in the membrane can be adjusted to either side of the bistable threshold to trigger assembly or disassembly of the clathrin coat.

Commented [EG10]: Do we need a citation here?

Commented [MJ11]: Here, what is the bistable threshold?

To characterize the dynamical properties of our oscillatory model and evaluate its experimental realizability, our study is organized as follows: describe the viable oscillatory parameter space as informed by biologically realistic kinetic parameters; explain model reductions and analysis; interrogate the period and amplitude tunability; measure parametric and noise robustness; compare nonspatial modeling results to a spatial reaction-diffusion simulation; demonstrate how the protein oscillations can be coupled to higher-order self-assembly; and finally, discussion of significance to experimental synthetic biologists.

Model and Methods paragraph— Building upon the fundamental mechanisms of clathrin-coat assembly, we present a straightforward model for a biochemical oscillator that capitalizes on the dynamic regulation of membrane localization to induce the necessary nonlinear behaviors for oscillations. Our model incorporates five initial species derived from clathrin-mediated endocytosis (CME), engaging in interactions both on and off the membrane while conserving total mass. Two enzymes, a lipid-modifying

kinase and phosphatase, operate in opposition to regulate the membrane's phosphorylation state. The membrane composition is represented as a combination of phosphorylated PIP2, which facilitates the localization of cytosolic proteins, and unphosphorylated PIP, which lacks such functionality. The extent of membrane localization and the accompanying enhancement of protein binding are determined by the ratio of PIP2 to PIP at any given time. The membrane localization of enzymes occurs indirectly through an adaptor protein AP2, which possesses a lipid binding interface specific to PIP2.

This is a result paragraph: The model possesses oscillatory potential for two reasons. First, the enzymes control the degree of membrane localization, and thus binding enhancement, for all species in the system, including the enzymes themselves. This means that enzymes accelerate or decelerate their own activity as a function of their dynamic equilibrium on the membrane, producing ad-hoc cooperativity and nonlinear feedback in the form of an opposing positive and negative feedback loop. Second, this nonlinear feedback is mediated through an intermediate adaptor protein. Intermediates are necessary to delay the feedback so that oscillatory overshoot and undershoot of the steady state is possible. Additionally, the adaptor intermediate feeds the input (PIP2/PIP ratio) incoherently to both enzymes, which has been shown to enhance oscillatory robustness.

As a final summary of our model, high PIP2 concentration recruits more adaptors to the membrane, which recruits both kinase and phosphatase. Kinase binding affinity is enhanced in 2D search space and converts more PIP into PIP2, causing more recruitment through positive feedback. Phosphatase experiences the same enhancement, reducing the amount of PIP2 and membrane localization and using the momentum from the positive feedback to amplify the negative regulation. Through correct tuning of the strength of these two feedback valences (positive feedback must happen faster than negative feedback), the system produces periodic excitation and relaxation in the concentrations of all species.

Commented [EG12]: Is this needed?

Commented [MJ13]: We discussed how it is not actually symmetric, since AP2 does not bind to PI(4)P, so this seems a bit misleading, I'm not sure what the symmetry refers to.

Commented [JF14R13]: Perhaps talk about asymmetry of the system in more detail here

Commented [EG15]: Are you sure this is true for our system? Have we run any simulations of {"K"+"L"<->"LK","LK"->"K"+"Lp","Lp"+"P"<->"LpP","LpP"->"L"+"P","K"+"Lp"<->"LpK","L"+"LpK"<->"LpKL","LpKL"->"Lp"+"LpK","Lp"+"P"<->"PLp","Lp"+"PLp"<->"LpPLp","LpPLp"->"L"+"PLp"}
LEARN does not rule out oscillations or bistability with this

Commented [MJ16R15]: I see, the point here is to allow the enzymes themselves to localize to the membrane and then use dimensional reduction to drive catalysis without using AP. But these enzymes have to each have two binding sites. It still effectively has intermediates in it.

Commented [EG17]: What do you mean by incoherently?

Commented [EG18]: I think this should be its own paragraph.

Commented [EG19R18]: Or maybe we should somehow explain it better in the area above so this does not need to be here

MODEL and METHODS

2.1 Model Description: Our model contains 5 monomeric species, an adaptor protein A, a phosphatase P, a kinase K, and lipids that exist in two states, unphosphorylated L (e.g. PI(4)P), and phosphorylated Lp (e.g. PI(4,5)P_2). They react with one another via only bimolecular and unimolecular reactions, with 5 distinct reversible binding reactions and two distinct (irreversible) catalytic reactions (Fig 1). We model the reaction network primarily using mass-action kinetics solved using systems of nonlinear differential equations, supplemented by non-spatial stochastic simulations using the Gillespie algorithm. We also quantitatively map the reaction parameters for spatial stochastic reaction-diffusion simulations solved using the NERDSS software. The proteins $A, K,$ and P each have two binding interfaces, one for a lipid (either L or Lp), and the other for a protein, where A can bind to either K or P using its interface, so it cannot bind both simultaneously. The lipids each only have a single interface for binding proteins, but they can be catalytically converted to the other state by the appropriate enzyme. We can thus form complexes with 2-4 monomer species, producing 16 distinct species total.

Chemical Mass Action Kinetics and Nonlinear ODE Formulation

We formulated the model reactions using chemical mass action kinetics, a widely accepted framework for modeling biochemical reaction systems. This approach describes the reaction rate as a product of the reactant concentrations raised to the power of their stoichiometric coefficients. We made the typical assumption of mass action, while also incorporating additional assumptions specific to modeling the membrane localization effect. For the membrane localization, 2-dimensional versions of 3-dimensional reactions have their forward rate constant scaled by volume-to-area ratio divided by a length scale to

make it dimensionless, which from this point on will be referred to as the dimensionality factor DF. We represented the reaction system as a set of nonlinear ordinary differential equations (ODEs), capturing the dynamic behavior of the system over time.

Modeling 2D reactions with mass action kinetics

Commented [EG20]: All the random floating letters presumably from equations need to be dealt with :/

Although our reaction system includes (i) 3D-3D binding, (ii) 3D-2D binding, and (iii) 2D-2D binding interactions, we model all species as bulk concentrations with the typical V^{-1} units of μM and all binding rate constants with units $\mu M^{-1}s^{-1}$. This is done by defining the dimensionality factor DF:

$$DF = \frac{V}{A \cdot h} \tag{1}$$

which for a reaction pair, relates a 3D binding constant to its effective 2D counterpart on the membrane while maintaining 3D units:

$$k_f^{mem} = DF \cdot k_f^{3D} \tag{2}$$

where k_f^{mem} is the effective 2D membrane-localized rate constant but converted to 3D units of $\mu M^{-1}s^{-1}$; k_f^{3D} is the 3D bimolecular rate constant of the same pair of reactants in solution, also with units of $\mu M^{-1}s^{-1}$; $\frac{V}{A}$ is the volume-to-area ratio of the reaction system, with units of length; and $h = \frac{k_f^{3D}}{k_f^{2D}}$, where k_f^{2D} is the association rate in 2D (units of A/time), is a length-scale specific to a particular pair of reactants that relates the 2D binding rate to the 3D binding rate.

DF is therefore a dimensionless scaling parameter that allows us to easily model the rate of a membrane-localized reaction as simply its rate in solution, multiplied by DF. Importantly, DF captures two reaction properties necessary for translating a reaction rate from 3D to 2D in a non-spatial model: **(i)** the volume-to-area ratio, which encodes the macroscopic effect at the bulk reactant concentration level of mapping

2D area densities to 3D volume densities; **(ii)** h, which encodes microscopic effect at a single reaction event of the different binding properties between 3D and 2D domains.

The length scale h is related to a thermodynamic property specific to a pair of reactants if we assume that the unbinding kinetics are independent of dimensionality, i.e. $k_r^{2D} = k_r^{3D}$. We make this assumption, and given that $K_{eq}^{2D} = \frac{k_f^{2D}}{k_r^{2D}}$ regardless of dimension, we have:

$$h = \frac{k_f^{3D}}{k_f^{2D}} = \frac{K_{eq}^{3D}}{K_{eq}^{2D}} \quad (3)$$

where, K_{eq}^{3D} and K_{eq}^{2D} are the 3D and 2D equilibrium constants.

As 3D binding rate constants and equilibrium constants have units in terms of volume, while their 2D counterparts have units in terms of area, their ratios give h units of length. Empirical measurements of h place it at the nanometer scale, with measurements from 1nm up to even 100nm. For our nonspatial model, h is not a free parameter and is not explicitly included in our rate equations; instead, the combined effects of h and the system geometry $\frac{\mathrm{V}}{\mathrm{A}}$ are modeled together within the dimensionality factor DF.

However, we do implicitly consider the typical length scales of h when choosing values of DF to perform parameter sweeps against, in order to keep $\frac{\mathrm{V}}{\mathrm{A}}$ within physiological values expected for eukaryotic cells (~ R/3 or ~1-10um). For spatial simulations, h, V, and A are all separately specified.

TERMINOLOGY

For the rest of our optimization and analysis pipeline, we use the following biologically-inspired nomenclature to refer to model inputs and outputs, and to nicely comport with our evolutionary optimization method: The full list of model input parameters and initial concentrations are listed out in another table.

Term	Definition

Commented [EG21]: This seems unnecessarily verbose. Not sure though what to have instead

Commented [EG22]: We'll have to deal with this when talking about experimental since I used a different range I think

Commented [MJ23R22]: It should be 1-10um, V/A is approximately R/3, and Eukaryotes have radii in wide ranges, from R~2um to 50um.

Commented [EG24]: Since this has not been introduced yet, maybe we have terminology after an introduction

Commented [EG25R24]: Going back to this, since you also mention the optimization when talking about truncating the solutions for measurements, I think it may be worthwhile to have a brief intro at the beginning give a summary of everything in this more technical section

Commented [MJ26]: We do need a table of all parameters and initial conditions.

genotype	The array of rate constants and initial concentrations that are mutated, recombined, and selected during optimization, defining a point in genotype space
phenotype	The period and amplitude of the resulting periodic solution
individual	The combined genotype-phenotype combination
population	The collection of genotypes that is evolved during optimization, or the collection of individuals that define the solution space during analysis

2.2 Solving the system of ODEs numerically

Our system of ODEs has 16 time-dependent variables interacting via 19 reversible reactions and 6 catalytic reactions. Monomers: A, K, P, L, Lp, dimers: AK, AP, LpA, LpP, LK, three-mers: LpAK, LpAP, AKL, and APLp, and 4-mers LpAPLp and LpAKL represent the concentrations of the complexed and noncomplexed forms of the chemical species in our model. Four mass conservation laws constrain the fixed total concentrations of lipid, adaptor protein, kinase, and phosphatase.

$$Lipid_{total} = L + Lp + LK + LpP + LpA + LpAK + LpAP + 2LpAKL + 2LpAPLp + APLp + AKL \quad (4a)$$

$$A_{total} = A + LpA + LpAK + LpAP + LpAKL + LpAPLp + AK + AP + APLp + AKL \quad (4b)$$

$$K_{total} = K + LK + LpAK + LpAKL + AK + AKL \quad (4c)$$

$$P_{total} = P + LpP + LpAP + LpAPLp + AP + APLp \quad (4d)$$

Reaction network: Our reaction network contains twelve tunable kinetic parameters, plus the dimensionality factor (DF). Our five reversible dimerization reactions use 5 distinct forward rates k_f^m, and

Commented [MJ27]: This is the full model that incudes all possible intermediates, so I added the missing two AKL and APLp species to the equations below. We have to be explicit if we want to talk about the 'simplified' model where we start with only 12 variables, so mass conservation reduces it to 8.

Commented [MJ28R27]: I also added the stoichiometric factors, which are necessary.

5 distinct reverse rates k_r^m, where m indicates which reactant monomers participate. We have two catalytic k_{cat}rate constants, k_{cat}^P and k_{cat}^K for enzymes P and K. We assume no cooperativity in the reactions as monomers combine to form intermediates, aside from the changes that must emerge due to dimensional reduction. The five dimerization reaction rates apply for the bimolecular reactions involving higher order intermediates. Similarly, the catalysis rate for the enzymes K and P are identical regardless of whether it is bound to another protein. All reactions that produce the 4-mers use the same rates as the interfaces involved in the dimer reactions, but converted to 2D values via the *h* lengthscale, as they all occur on the membrane. Thus We also assume the *h* lengthscale is the same for all 2D reactions, although in reality it can vary between pairwise species, although not without constraints due to thermodynamic cycles in our model (see SI). We also assume that dimensional reduction only changes the on-rates, and not the off-rates of the reactions, when in reality it can affect both. These simplifications allow us to limit the size of our already large parameter regime.

Restricted model: This model restricts the adaptor protein A such that it can only bind to enzymes after lipid binding. some of the reactions to simplify the number of species. It only has 12 variables, and with mass conservation reduces to 8.

The general form of our system of ODEs can be represented in the form:

$$\dot{\boldsymbol{c}}(t) = f(\boldsymbol{c}(t), k;\ DF) \tag{5}$$

where:

- c $\in R^{16}$ repret the concentration vector of the biochemical species involved in the system at time ċ(t), and ċ is its time derivative, indicating the rate of change of these concentrations.
- k $\in R^{12}$ is the vector of tunable kinetic parameters that parameterize the reaction rate laws.

- DF is the dimensionless scalar value that scales the rate laws of membrane-bound reactions, and is treated as a fixed feedback or gain parameter during optimization. In the spatial simulations, the three parameters in the DF: V, A, and h, must be specified individually, as we explicitly capture diffusion and species positions in both 3D and 2D.

The timespan for numerical solution was set to 2000 seconds, estimated to accommodate the longest anticipated oscillation period. This estimation was based on the slowest timescale within the system's dynamics, which is inversely related to the slowest reaction rate. Mathematically, this was approximated by $T_{max} \approx min\left(\frac{1}{k_i c_i}\right)$, where k_i are the rate constants and c_i are the concentrations of the species involved. This expression identifies the slowest reaction by considering the minimal value of the product of concentrations and the reciprocal of rate constants, providing a rough estimate of the upper limit of oscillation periods within the system. This does mean that we will not detect oscillators with a period slower than 1000s, but for our purposes we consider this a sufficient range. To sample slower times, we would need to extend this window, which would increase computational expense during large parameter sweeps.

In our numerical integration approach, the Rodas5P method was utilized. Rodas5P is an implicit Runge-Kutta solver that is particularly well-suited for efficiently solving stiff or periodic systems. This is because it retains the desirable conservation properties of implicit methods like backwards differentiation (BDF), but is a single step rather multistep integrator, allowing for easy adaptive time-stepping (Steinebach, 2022) . As such, dynamical systems such as ours that feature rapid changes in reactions rates can be stably solved for without the computational expense of smaller timesteps or higher order methods.

Commented [EG29]: Is this detail needed? I don't know the significance/how well know this family is to really make a judgement

Commented [EG30R29]: Otherwise I can just put "that" to get better flow

Computing the solution phenotype

Although we solve for all the ODE variables not eliminated through mass conservation, we measure the phenotype of a solution from the observable A_{mem}. This is a measure of A species localized to the membrane relative to the total A in the system, and is a unitless fraction. For the restricted model:

$$A_{mem}^{res}(t) = \frac{LpA(t) + LpAK(t) + LpAP(t) + LpAKL(t) + LpAPLp(t)}{A_{total}} \quad (6a)$$

For the full model:

$$A_{mem}(t) = \frac{LpA(t) + LpAK(t) + LpAP(t) + LpAKL(t) + LpAPLp(t) + AKL(t) + APLp(t)}{A_{total}} \quad (6b)$$

A_{mem} is a relative measure independent of the total mass and initial conditions, and provides a normalized index suitable for comparative analysis of oscillatory behavior across different parameter sets and initial conditions, ensuring a measure of the dynamical properties rather than absolute concentration values.

We also truncate the resulting solution array A_{mem} to the last 90% of the saved time points, as we found that helped our optimization pipeline to avoid getting stuck in regions of dampened oscillations.

The period and amplitude of A_{mem} are measured to characterize the oscillatory behavior of a given individual, computed with the following expressions:

$$\text{per}(A_{mem}) = (t_{\text{peak},n} - t_{\text{peak},n-1}) \quad (7a)$$

$$\text{amp}(A_{mem}) = A_{\text{mem}}(t_{\text{peak},n}) - A_{\text{mem}}(t_{\text{trough},n}) \quad (7b)$$

2.2 Genotype optimization and exploration

To generate solutions with stable oscillations, we optimized the model inputs, or genotypes, using a genetic algorithm (GA). GAs are a class of stochastic gradient-free optimization algorithms inspired by the process of natural selection, which evolve a population of candidate solutions towards an optimal or near-optimal solution. The genetic algorithm optimization allowed all parameters and initial conditions to vary within physiological ranges (though subsets were fixed for certain downstream analyses of solution space). By iteratively applying selection, crossover, and mutation operators, we were able to efficiently

Commented [EG31]: IMPORTANT: I am 99% confident that you made the same mistake as the original genetic oscillator paper. This is a telescoping series and will simplify to 1/(n-1) * (final t - first t)

Commented [MJ32R31]: Ezra is again correct about this, it is equivalent to measuring the distance between the first and last peak and dividing by the number of peaks present (minus 1)

Commented [EG33]: This equation is not telescoping :) Not sure why absolute value bars are needed though if it knows that it is a peak time vs a trough time...

Commented [EG34]: I am unsure what you mean by this.

search the parameter space and identify regions of parameter space that yielded oscillatory behavior.

Rate constants	Range
$\boldsymbol{k_f}$ (binding rate)	0.001 – 10 $\mu M^{-1}s^{-1}$
$\boldsymbol{k_r}$(unbinding rate)	0.001 – 1000 s^{-1}
$\boldsymbol{k_{cat}}$ (catalytic rate)	0.001 – 1000 s^{-1}

Species	Range
PIP/PIP2	0.1 – 100.0μM
PIP5K	0.001 – 100.0μM
Synaptojanin	0.001 – 100.0μM
AP2	0.001 – 100.0μM

For our parameter sweep, we had to choose certain hyperparameter values for our GA that would maximize both the quality of saved individuals and coverage of the search space. These hyperparameters were the population size, crossover rate, mutation rate, mutation scalar (explained in the mutation section), and number of tournament groups the population would be divided into for selection. We conducted a hyperparameter sweep via grid search where we varied a single hyperparameter while holding all others at nominal values, using the same seed to control for the stochasticity of the GA.

The results of the hyperparameter sweep are shown in Figure S2, where the performance metrics were max-pairwise distance in the final population to measure search coverage, and average fitness of the final population to measure search quality. Our conclusion from this analysis was that population size was by far the most important hyperparameter and dominated the effect of any variation in the other hyperparameters. Therefore, we chose a population size of 100,000, which was the maximum feasible size within our computational constraints.

The initial population P is generated by sampling 100000 genotype vectors $g_j = [k_{j,1}\, k_{j,2} \cdots k_{j,n}]$where each gene element of genotype g_j is sampled log-uniformly:

$$k_{j,i} = 10^{Uniform(log_{10}(min\,(k)),\, log_{10}(max\,(k)))} \quad \text{for i} = 1, 2, \ldots, \text{n and j} = 1, 2, \ldots, \text{m} \qquad (8a)$$

and concatenated into the population matrix P:

Commented [EG35]: You might want to change this to rho or some other letter to prevent confusion with the Synaptojanin concentration P.

Commented [EG36R35]: The only issue with rho is that generally we like to use uppercase letteres for matrices, so maybe some other letter could work

$$\mathrm{P} = \begin{bmatrix} k_{1,1} & \cdots & k_{1,n} \\ \vdots & \ddots & \vdots \\ k_{m,1} & \cdots & k_{m,n} \end{bmatrix} \tag{8b}$$

where n is the number of genes in a genotype, lb_i and ub_i are the lower and upper bounds for i-th gene of a genotype, and $\mathrm{m} = 100000$ for the number of genotype vectors in the population.

P is then transformed with mutation, crossover, and selection operations for every generation, for 5 generations total (not including the initialization).

Mutation

The chromosomal mutation rate (whether a vector is chosen to be mutated) was set high at 95% in order to encourage exploration and maintain population diversity.

If mutation is performed, we use the Polynomial Mutation (PLM) scheme, which is mathematically represented as:

$$c_i' = c_i + \Delta \cdot \delta_i \tag{9a}$$

where c_i' is the mutated i-th gene, c_i is the original value of the i-th gene, Δ (Delta) is the mutation range (set to 1.0 by default), and δ_i is the mutation factor determined by:

$$\delta_i = \begin{cases} 2u_i^{\frac{1}{\eta+1}} - 1 & \text{if } u_i \leq 0.5 \\ 1 - (2(1-u_i))^{\frac{1}{\eta+1}} & \text{if } u_i \geq 0.5 \end{cases}$$

where u_i is a uniform random number in [0,1], and η (eta) is the distribution index (set to 2 by default). Each gene has a probability pm = 0.75 of being selected for mutation.

This mutation scheme introduces variability in a controlled manner, with the distribution index η determining the likelihood of creating solutions near or far from the parent. Lower values of η allow for more distant mutations, while higher values tend to create offspring closer to their parents. The scheme

allows for both exploration and fine-tuning of the solution space, maintaining genetic diversity and preventing premature convergence.

Crossover

Crossover was performed at a rate of 75% using the Simulated Binary Crossover (SBX) mechanism to all sets of parents. Parents are adjacent individuals stored in the population matrix. SBX creates two offspring that are centered around their two parents in the decision space, with a spread that is proportional to the distance between the parents.

The crossover operation can be mathematically represented as:

$$c_1 = \mu - \beta c$$

$$c_2 = \mu + \beta c$$

Here $\mu = (v_1 + v_2)/2$ represents the mean of the parent vectors and $c = (v_1 - v_2)/2$ is half the difference between parents. The spread factor $\beta = (2URN)^{(1/(\gamma+1))}$ when URN ≤ 0.5, or $\beta = (2(1-URN))^{(-1/(\gamma+1))}$ when URN > 0.5, where URN is a uniform random number in [0,1). The distribution index γ is set to 2 by default, and each component has a probability pm = 0.3 of being recombined.

This crossover scheme allows for both exploration and exploitation of the search space. The distribution index γ controls how similar the offspring are to their parents - a larger γ produces offspring closer to the parents, while a smaller γ allows for more diverse offspring. This mechanism is particularly effective for real-valued optimization as it preserves the average of the parent values while allowing for controlled variation in the offspring.

Selection

For the selection process, tournament selection was utilized. This method involves randomly selecting multiple subsets of individuals from the population and then choosing the fittest individual from each to be a part of the next generation. The primary advantage of tournament selection is its balance between maintaining diversity within the population and ensuring the propagation of the fittest individuals, and is less susceptible to premature convergence compared to other selection strategies (Xie & Zhang, 2012). We chose a tournament size of 5% of the overall population, dividing the total population of 100,000 individuals into 20 groups of 5000 individuals every generation.

Hyperparameter (units)	**value**
Mutation rate per individual	0.95
Mutation probability (pm) per gene in an individual	0.75
Sampling parameter: Mutation distribution using Polynomial Mutation Scheme with parameter η	2
Sampling parameter: Mutation range (delta)	1.0
Crossover rate for an individual (in addition to mutation)	0.75
SBX probability (pm): probability of choosing a gene in an individual	0.3
SBX distribution index (γ)	2
Tournament group size (# of individuals)	5,000
Population size (# of individuals)	100,000

Genetic algorithm compared to alternative search methods

This decision to employ a GA compared to alternative optimization methods was predicated on several key advantages of GAs in handling our problem type. Firstly, GAs are renowned for their ability to

effectively navigate and search through high-dimensional and non-linear parameter spaces, characteristics inherent to our biochemical oscillator model (Dorsey & Mayer, 1995). Unlike gradient-based or point-to-point search methods, GAs operate by simulating the process of natural evolution, thus providing a robust mechanism for identifying global optima in a landscape potentially riddled with local optima. This attribute is particularly valuable in our study, as the parameter space of the biochemical oscillator is complex and the optimal regions are not readily apparent.

Fitness function

The fitness function for assigning scores to oscillatory behavior used properties of the real-time ODE solution $A_{mem}^{res}(t)$ and its discrete Fourier transform, $F_\omega[A_{mem}^{res}(t)\,](\omega)$. We found empirically that for lower DF, we found larger solution sets using $A_{mem}^{res}(t)$, but for the analysis of the oscillator amplitudes, we report values from the full species $A_{mem}(t)$.

For all solutions $A_{mem}^{res}(t)$, we evaluate their discrete Fourier transform $F_\omega[A_{mem}^{res}(t)](\omega)$ using the built-in Julia function rfft. We calculate the one-sided complex modulus of the DFT. To speed up the computation, we use slightly fewer data points (N=19,683) than the 20,000 point real-space vector, and normalize the resulting DFT array by half its length (N/2). Given the numerical complex modulus, we use the built-in finite difference peak finder algorithm (using default parameters) to identify N_P peaks in the spectrum. For each *i* peak we evaluate its amplitude γ_i, and its sharpness s_i. The value s_i reports the standard deviation of the peak height at its maximal amplitude compared to the amplitude at the neighboring point on either side. We ignore peaks with a height <1E-2. A larger standard deviation indicates a more distinct peak, suggesting a stronger and more stable oscillatory behavior. We then calculate the fitness, we are trying to maximize, using

$$f\left(F_\omega[A_{mem}^{res}(t)](\omega)\right) = \sum_{i=1}^{N_P} s_i + \sum_{i=2}^{N_P} (|\gamma_i - \gamma_{i-1}|) \qquad (10)$$

Commented [EG37]: I don't see how simulating evolution ->robust mechanism. Just say that it is better at determining global optima when there are many local optima (if that is true, in which case we want a citation). Also, you may want to better specify why we would want a global optima. If I remember correctly, there were not clear differences between oscillatory solutions with high fitness function values and those with low fitness function values

Commented [MJ38]: Update both of these sections to reflect what is done in your code that generated the data. Using a few sets of parameters, solve for Amem(t). Do the DFT, compute the peaks and the fitness. Send all this data to me to check using MATLAB.

Commented [MJ39R38]: Make sure you update all the steps that might involve filtering due to peak height or prominence.
Make sure you update the classification steps that decide if it is oscillatory, including number of peaks, peak prominence, etc.

Commented [MJ40R38]: After updating the text describing the fitness function. You will need to update the definition of Amem(t) in your code to include all species on the membrane. Then regenerate the data, since it will affect the amplitude, and should also impact the DFT and thus the fitness. It will not affect the period.

The second term selects for high-amplitude peaks at a single frequency. This function identifies short and long period oscillators, with a range of amplitudes. High fitness is highly predictive of undamped oscillators. These fitness values are used by the genetic algorithm to evaluate which individuals to breed, propagate, mutate.

Classifying solutions found by the GA for further analysis

To analyze the solutions found by the GA post-hoc, we do not store every solution, but instead just those that are classified as oscillatory. Instead of setting a threshold on f to discriminate oscillatory from non-oscillatory or damped-oscillatory solutions, we perform an additional analysis on the real-time dynamics of each individual. We evaluated the real-time behavior to filter out solutions with less than two identified peaks, eliminating them from our set of most-likely oscillatory solutions. Note this only affects stored solutions, not the evolutionary process. This means that the maximal period we will detect is <2000s; for slower oscillations, the time-range of the simulations would need to be extended. Peaks were identified with a first-order difference peak finder algorithm. If the amplitude of the oscillations in $A_{mem}^{res}(t)$ is less than 0.01, or 1% of the total amount of A, we also treat the solutions as non-oscillatory due to the weak signal. Finally, we look at the last 200 seconds (2000 values) of $A_{mem}^{res}(t)$ and evaluate the standard deviation. If it is <1e-6, this indicates the solution is at a steady state, and is non-oscillatory. The real-time analysis helps identify solutions most likely representative of oscillatory solutions over our period range of interest. For all solutions that pass this post-hoc real-time analysis, we save them as likely oscillatory solutions.

Commented [MJ41]: Just peaks now.

Commented [MJ42]: I just edited this-we are not using any prominence filter on the real-time solution anymore

RESULTS

3.0 AP2 is necessary for oscillations to be possible.

This also ablates DF dependence. Cite Tyson and Novak, and also show Ezra's results using the LEARN algorithm. (this LEARN was inconclusive for other ablations, because the algorithm doesn't have the membrane localized enzyme binding rate assumed to be the cytosolic rate scaled by DF, thinks it is independent rate)

Without AP2 binding, system reduces to kinase-phosphatase interconversion and no oscillations are possible (cite previous paper, this has been proven).

Without AP2, the network becomes symmetric, allows fixed point. Innate structural asymmetry that comes from Lp binding to both A and the kinase species (versus L which only binds to phosphatase species) creates a natural avoidance of this kind of stable fixed point.

3.1 Dimensional reduction is necessary to produce oscillations

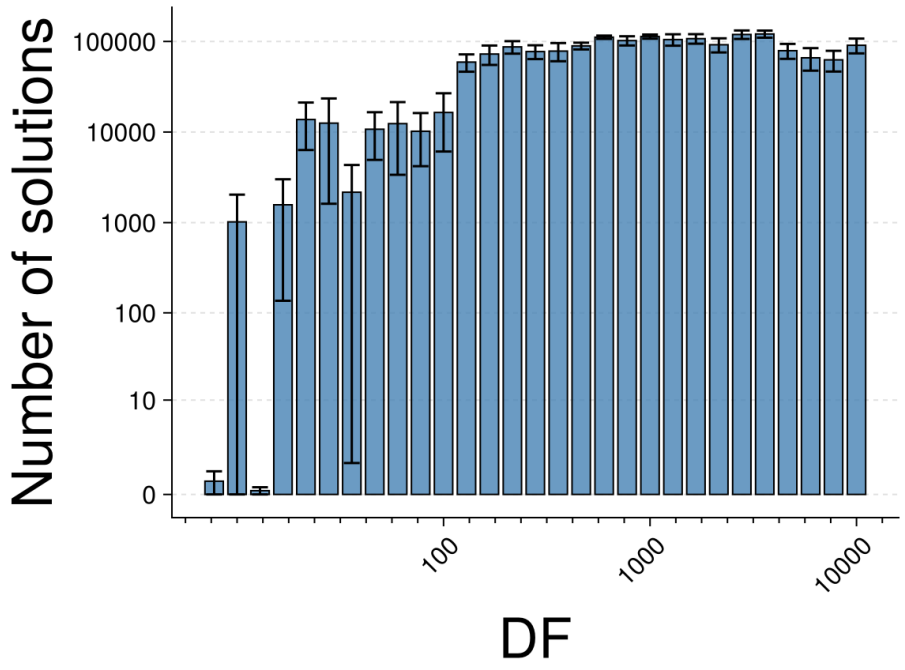

When we add AP2 into our model, the network is fundamentally asymmetric; Both AP2 and P compete to bind to the phosphorylated lipid Lp, whereas only K binds to the unphosphorylated lipid L. This network will produce oscillations, but we hypothesize that it requires dimensional reduction, or DF>1, to amplify forward (bimolecular) reaction rates for reactions occurring in 2D relative to 3D. Using global sampling, we do not find solutions when DF=1 for any parameter regime.

We performed model reduction, and reduced our system to two variables. In this reduced model, we can maybe? Show that DF=1 doesn't work if we make further simplifications to the asymmetry in the model.

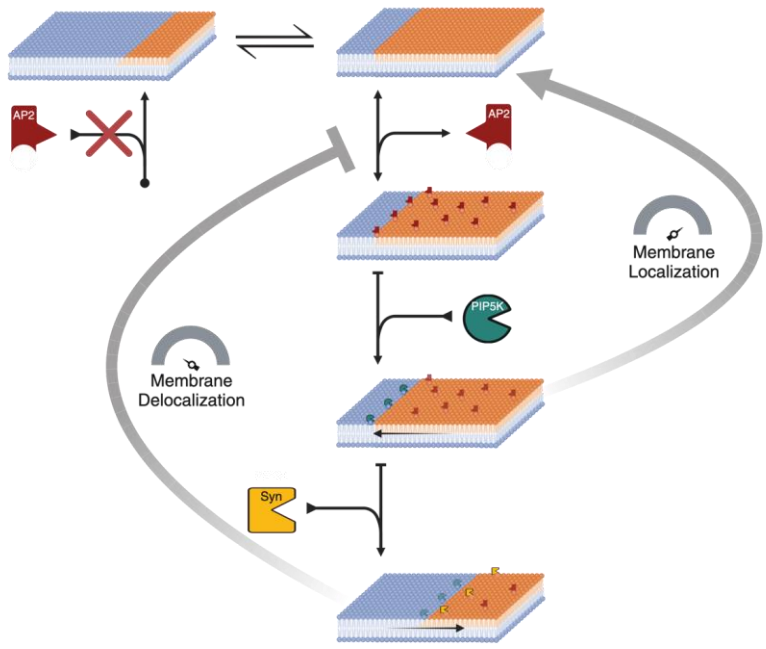

Figure 2. Illustration of the scenario where membrane localization has no effect on the reaction dynamics. When the dimensionality factor (DF) is set to 1.0, eliminating the difference in reaction rates between the membrane and the solution, the resulting rate laws and dynamics of the membrane-localized reactions are identical to those in the dilute phase. This indicates that the mere presence of membrane-bound complexes, without an enhancement in reaction rates, does not alter the overall behavior of the system.

First, we set DF=1.0, which eliminates the difference in reaction rates between the membrane and the solution, and thus $K_m^{4a} \equiv K_m^{4b}$ and $K_m^{5a} \equiv K_m^{5b}$. In this scenario, the enzymatic reactions occur at the same rate in both spatial compartments, but the formation of membrane-bound complexes can still influence the dynamics through sequestration. Under these conditions, no oscillatory solutions out of 500,000 samples were found during parameter optimization. This result suggests that the mere presence

of membrane-bound complexes as a potential sequestration mechanism is insufficient to generate oscillations.

Eliminating binding of A to the membrane prevents any dimensional reduction, and therefore eliminates oscillations

A key element of our model is that binding to A does not induce any cooperativity or changes in the action of the enzymes, simply via the protein-protein interaction. Thus, if A cannot bind to the membrane and bring the enzymes to perform a 2D search with their substrates, it does not impact the enzymatic reactions in any way. This model, similar to the model without A, cannot produce oscillations.

Eliminating binding between either enzyme and adaptor A prevents that enzyme from exploiting dimensional reduction

In this case, we are now allowing only one of the two enzymes to exploit dimensional reduction to amplify its binding to its substrate. We can do this by preventing the enzyme from binding to A, setting either k_f^{AP} or k_f^{AK} to zero. We can again perform global sampling in either of these cases, for fixed values of the DF=1, 10, 100, 500, 1000, 5000, 10000. Do we ever find oscillatory solutions? If you find solutions, check them to verify whether they oscillate or not. Document in the methods exactly what you do for this global sampling.

We use model reduction to see if we can show whether or not these oscillations are possible.

Other sources of asymmetry between the enzyme reactions can drive oscillations with less dramatic DF enhancement

- **Asymmetry between** k_f^{AP} and k_f^{AK} changes recruitment to the membrane. We hypothesize that this is similar to creating **asymmetry in the concentration of K and P**.

- **Asymmetry between** k_f^{LpP} and k_f^{LK} changes the binding of enzymes to substrate.
- **Asymmetry between** k_{cat}^{LpP} and k_{cat}^{LK} changes the catalysis rates of enzymes to substrates.

To get oscillations with a low DF=50, or DF=100, key asymmetries between the enzyme activities must be amplified by asymmetries in concentrations??

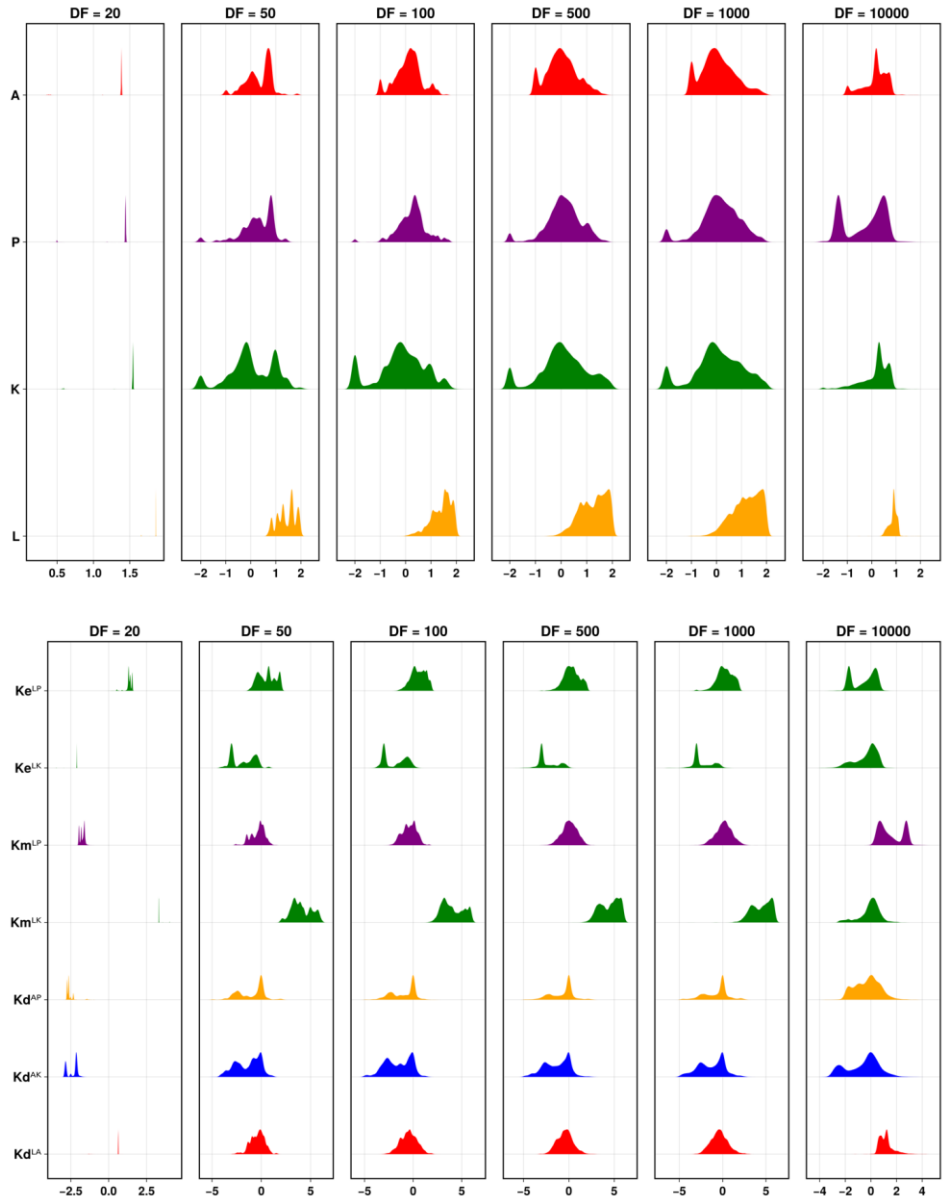
DF = 20
DF = 50
DF = 100
DF = 500
DF = 1000
DF = 10000
A
P
K
L
Ke^{LP}
Ke^{LK}
Km^{LP}
Km^{LK}
Kd^{AP}
Kd^{AK}
Kd^{LA}

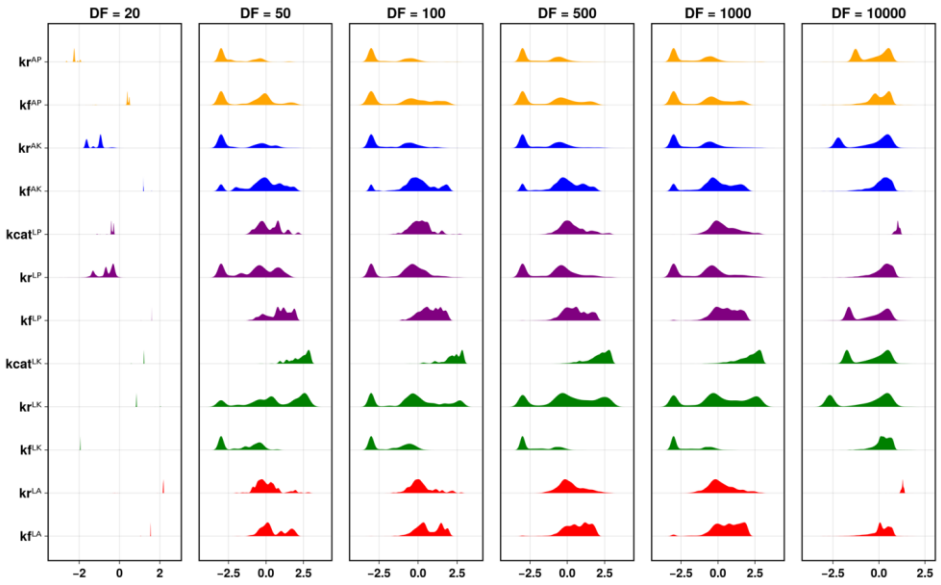

Figure 4. Solutions found from global sampling with fixed DF values illustrate asymmetries are most pronounced in the K_m values for the two enzymes with their substrates. The solution space increases with DF, with far more solutions more readily identified.

DF can compensate for inadequate kinetic asymmetry between kinase and phosphatase (Sweep results from reference symmetric regime…)

Theory on Rate Limitation Criteria in the Lipid Oscillator Model

Reference Regime: We begin by considering a reference regime where:

- Total amounts of kinase (K) and phosphatase (P) are equal, and their catalytic rate constants are identical.
- The system starts with all the lipid in the unphosphorylated L state.
- The key asymmetry in the system arises from the faster binding of the phosphorylated lipid-adaptor complex LpA to kinase (K) compared to phosphatase (P) (i.e., kfAK > kfAP).

In this regime, the system is set up to favor kinase activity initially, but both enzyme activities (phosphorylation by K and dephosphorylation by P) are allowed to compete dynamically. The crucial difference lies in how the system's positive and negative feedback loops interact to drive oscillatory or damped behavior.

Core Theory: At the heart of this system is a positive feedback loop driven by kinase activity, which converts L to Lp, and an associated negative feedback loop driven by the complex formation of LpAP and its binding to Lp. The dynamics of LpAP and its interaction with Lp are critical in determining whether the system exhibits stable oscillations or settles into a steady state.

The key rate limitation criteria revolve around the balance between the positive feedback from kinase-driven Lp production and the negative feedback from the depletion of LpAP via its binding to Lp. Oscillations occur when the system introduces a temporary rate limitation in LpAP's ability to respond to the accelerating Lp production, which creates the necessary hysteresis to drive the system away from a steady state.

Positive Feedback Mechanism:

1. Initial Kinase Activity:
    - Starting with all lipid in the L state, kinase activity quickly converts L to Lp. As Lp forms, it begins to interact with adaptor protein (A) to form the complex LpA.

2. Formation of LpAK:
    - Because LpA binds faster to kinase (K) than to phosphatase (P) (due to kfAK > kfAP), a significant fraction of LpA forms the complex LpAK. This complex, LpAK, shares the catalytic activity of K but with an increased binding affinity for L due to the effect of membrane localization (represented by the DF factor).
    - The formation of LpAK amplifies the kinase-driven production of Lp, creating a positive feedback loop: more Lp leads to more LpA, which leads to more LpAK, further increasing Lp production.
3. Acceleration of Lp Production:
    - As Lp production accelerates, LpA formation also accelerates, reinforcing the positive feedback loop.

Negative Feedback via LpAP and Its Response to the Positive Feedback:

4. Formation of LpAP:
    - LpA, in addition to binding to K to form LpAK, also binds to P to form LpAP. However, the binding rate of LpA to P is slower than to K, meaning that LpAP formation lags slightly behind LpAK.
    - As LpAP forms, it acts as part of the negative feedback loop by binding to Lp to form the complex LpAPLp, which dephosphorylates Lp back into L.
5. Direct and Indirect Feedback Pathways:
    - The depletion of LpAP via its binding to Lp (i.e., LpAP + Lp → LpAPLp) is a direct feedback mechanism that is strongly amplified by the accelerating Lp production. As Lp levels rise, this depletion term is directly coupled to Lp's concentration, and the rate of LpAP depletion increases rapidly.
    - In contrast, the formation of LpAP is driven by more indirect feedback mechanisms, which include:

i. The regeneration of LpAP from the catalytic turnover of LpAPLp (i.e., LpAPLp → L + LpAP).
ii. The formation of LpAP from LpA binding to P (i.e., LpA + P → LpAP).

- These indirect pathways have intermediate steps and respond more slowly to the changes in Lp concentration compared to the direct depletion pathway.

6. Rate Limitation Criteria:
    - As the positive feedback loop accelerates, a rate imbalance develops: the negative feedback term (depletion of LpAP) becomes amplified more rapidly than the positive feedback terms (formation and regeneration of LpAP).
    - When the rate of LpAP depletion overtakes the rates of LpAP formation and regeneration, LpAP becomes rate-limited—its depletion accelerates faster than it can be replenished. This momentary rate limitation causes d(LpAP)/dt to dip negative, creating a delay or hysteresis in the system.
    - This temporary depletion of LpAP allows Lp to accumulate unchecked, setting the stage for the next phase of the oscillation.

Differentiating Damped and Oscillatory Solutions:

- Damped (or No Oscillation) Regime:
    - In damped solutions, the rate limitation in LpAP occurs too late to introduce the necessary delay before d(Lp)/dt turns negative. The positive and negative feedback loops remain too synchronized, allowing the system to quickly stabilize toward a steady state.
    - d(LpAP)/dt remains positive throughout the positive feedback phase, meaning LpAP is never sufficiently rate-limited. As a result, the system remains balanced, and no oscillation occurs.
- Stably Oscillatory Regime:

- In oscillatory solutions, d(LpAP)/dt experiences an inflection point during the positive feedback phase, where the depletion of LpAP overtakes its formation and regeneration. This dip introduces a rate limitation in LpAP, which allows Lp to accumulate beyond what the system can immediately regulate.
- The timing of this rate limitation is critical: it occurs before d(Lp)/dt turns negative, creating a necessary delay or hysteresis that pushes the system away from a steady state and into an oscillatory cycle.
- As LpAP regenerates later, the system transitions into the next phase of the oscillatory cycle, with alternating periods of strong positive feedback and negative feedback.

Conclusion: The balance between direct and indirect feedback mechanisms governing LpAP dynamics is crucial for determining whether the system exhibits stable oscillations or settles into a steady state. Oscillations occur when LpAP becomes rate-limited in time, allowing for a temporary imbalance in the feedback loops. In contrast, when the feedback loops are too synchronized, the system is damped and stabilizes without oscillating. This theory underscores the importance of timing and rate limitation in complex biochemical networks, where feedback-driven dynamics can lead to rich oscillatory behavior.

Without dimensional reduction, the model dynamics converge to a single asymptotically stable fixed point.

Ezra has shown that if you use a reaction network that has no adaptor proteins, so therefore all you have are lipids that can exist in two states and can be switched between them via a kinase and a phosphatase, you do not see oscillations.

If you have the adaptor present, but the DF=1, the only thing you've added to the model compared to the above is the formation of some intermediates that involve A, in particular A can sequester Lp by binding to it. However, this potential sequestration already makes the network too complex to be analyze (look up opposing enzyme networks with competitive inhibitor)

What if only one of the enzymes can exploit dimensional reduction? Empirically it appears to be that you cannot get oscillations if only one enzyme exploits dimensional reduction. However, analysis of the reaction network was not conclusive towards whether the system would be stable or unstable.

3.2 DF increases oscillatory solution space of high-frequency oscillations

The introduction of the dimensionality factor (DF) markedly expands the oscillatory solution space in our lipid-modifying enzymatic reaction network. DF acts as a critical scaling parameter, adjusting the 2D reaction rates on the membrane relative to the 3D rates in the solution. This adjustment effectively simulates the influence of membrane localization on reaction kinetics by multiplying the forward rate constants of membrane-bound reactions by DF.

This enhancement of membrane-bound reactions facilitates the formation of key complexes necessary for oscillatory behavior. For example, the formation of complexes such as LpAKL and LpAPLp, involving the kinase and phosphatase bound to the membrane, is crucial for maintaining the cyclic balance between phosphorylation and dephosphorylation. The increased formation of these complexes, driven by higher effective reaction rates, promotes a dynamic interplay among different species, leading to more robust oscillatory patterns.

Furthermore, DF promotes the formation of ternary complexes integrating adaptor proteins (AP2) with lipid-bound species. These complexes, such as LpAKL and LpAPLp, are essential for the sequestration of

PIP2 by AP2, a critical factor in sustaining oscillations. The increased occurrence of these complexes due to DF's modulation of reaction rates enhances the system's dynamic stability.

The scaling effect of DF also helps balance the positive (phosphorylation) and negative (dephosphorylation) feedback loops within the network. Properly tuned DF ensures that the phosphorylation rate by the kinase and the dephosphorylation rate by the phosphatase are harmonized, preventing runaway accumulation or depletion of PIP2 and stabilizing the oscillatory dynamics.

Additionally, DF impacts substrate competition, particularly between the kinase and AP2 for binding to PIP2. By adjusting membrane-bound reaction rates, DF influences the relative affinities of these interactions, ensuring that the sequestration effect of AP2 does not overpower the system's oscillatory capacity. This fine-tuning is crucial for maintaining oscillatory behavior across a broader range of parameter values.

Our simulations demonstrate that increasing DF broadens the oscillatory solution space, evidenced by the wider range of observed periods and amplitudes of oscillations. This expansion indicates that membrane localization, captured by DF, plays a pivotal role in facilitating oscillations by enhancing effective reaction rates and promoting the formation of critical complexes.

4.2 What criteria are no longer met as DF is dropped?

This will depend on likely many parameters at the same time, nonetheless, we can try to identify hypotheses and then test them, about inequalities or sets of inequalities regarding reaction fluxes (like kfLP*[P]tot) or parameter ratios (like kcatLP/kcatLK).

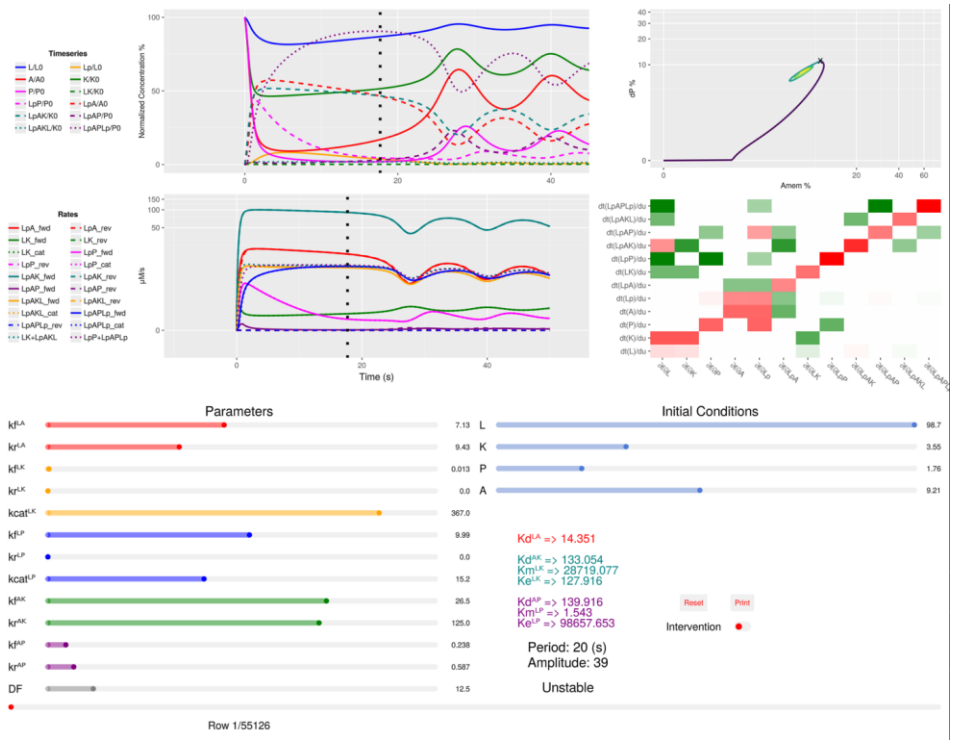

3.1 Mechanism of the Membrane-Associated Lipid Oscillator

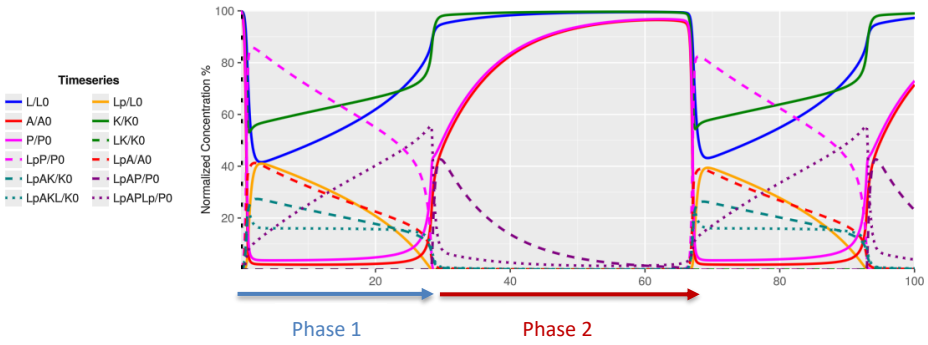

The primary dynamics of our lipid oscillator model can be divided evenly into two phases.

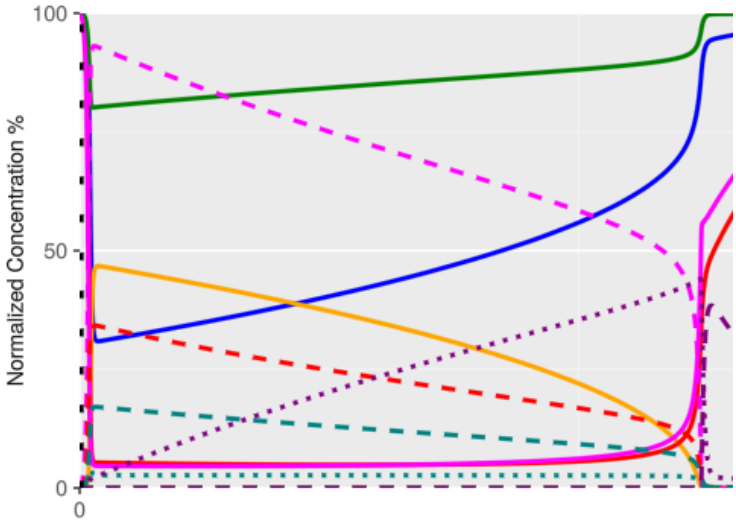

The first phase begins with high concentrations of Lp, LpP, LpA, and LpAK, while L, LpAP, and LpAPLp are present in low concentrations. Lp is bound and converted into L via LpAP at an increasing rate. Free LpA begins to dissociate into Lp and A due to free Lp depletion, which consequently destabilizes both LpAK and LpAP. However, this destabilization favors LpAP due to a structural asymmetry within the reaction network: disassociation of membrane-localized complexes releases free Lp, which binds to and stabilizes LpAP, but does not for LpAK. This asymmetry creates a fundamental advantage for phosphatase activity during this phase regardless of particular parameter values, precluding any steady state and necessitating an eventual depletion of free Lp given enough time.

The first phase concludes when Lp is fully depleted. LpA, LpP, and LpAK reach low but non-zero concentrations, and LpAPLp peaks.

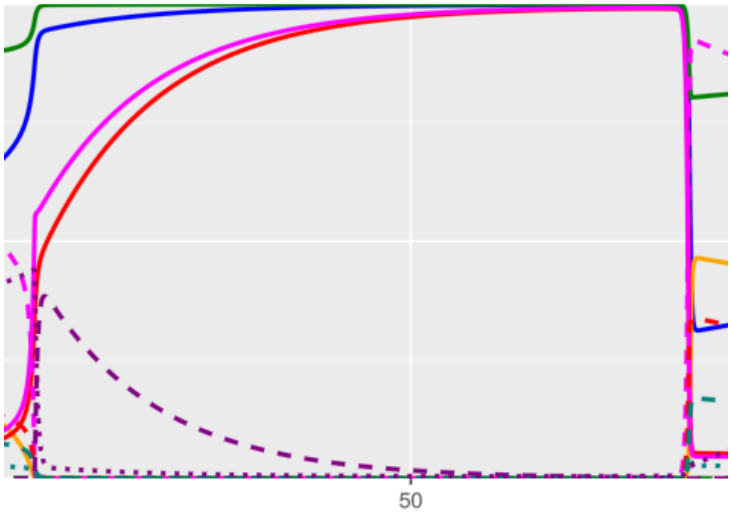

The transition from phase 1 to phase 2 begins with a dramatic shift in dynamics. As soon as Lp is extinct and can no longer bind LpAP to form LpAPLp, there is a shift in the dynamics. Free L, already increasing in phase 1, rapidly accelerates to a new plateau thanks to the high level of membrane-localized phosphatase paired with sudden removal of any LpAK formation which was previously mitigating its rise, due to Lp depletion. Free LpAP rapidly accumulates from near zero as LpAPLp turns over its already bound substrate but without any more ligand to rebind. LpAKL also decreases from a near constant amount in phase 1, dipping as its free from is destabilized and pushed towards disassociation. After this initial transition, the rest of the dynamics are dominated by the depletion of LpAP and accumulation of membrane-complex components; the components do not rebind, and the system experiences net delocalization and decomplexation. LpAP follows a steady depletion as it dissociates into LpA and P, and LpA then disassociating into Lp and A, upon which the released Lp is immediately bound and catalyzed by the remaining LpAP. Throughout this phase, L concentration slowly approaches maximum concentration, with nearly all lipid in the system as free L, and a small, decreasing amount remaining in

LpAP. Free A and P concentrations rise as LpAP dissociates, while K remains largely unbound due to lack of substrate.

Several mechanisms drive the second phase. LpAP acts as the primary inhibitor, effectively binding Lp released from LpAP/LpA dissociation even at low concentrations, preventing net formation of LpA or LpAK until LpAP is sufficiently depleted. A zero-order kinetics window emerges as remaining LpAP becomes saturated, creating a period where Lp consumption rate is independent of Lp concentration. This allows for transient Lp accumulation without immediate proportional increase in consumption. The catalytic balance is crucial, with LpAPLp turnover rate needing to be high enough to prevent Lp release from saturating LpAP again, suggesting a constraint on LpAPLp catalytic efficiency and LpAP unbinding rate. LpAP maintains a competitive advantage, outcompeting A and P in binding the small amounts of Lp released, key to maintaining its inhibitory effect. The system moves consistently towards LpAP depletion, with lack of Lp and saturation of L preventing significant back-reactions.

The critical transition at the end of phase 2 involves transient Lp accumulation as LpAP reaches its minimum, protected by the zero-order kinetics of saturated LpAP. Accumulated Lp binds to free A, forming LpA, which can then bind to either K or P. Even if LpAP formation is initially favored, LpAK can initiate positive feedback under certain conditions. For this to occur, LpAK must possess higher catalytic efficiency, faster product release, higher turnover number, greater stability, and access to higher substrate concentration compared to LpAP. If these conditions are met, LpAK can generate Lp faster than LpA or LpAP can consume it, establishing positive feedback and rapidly resetting the cycle.

As phase 2 concludes, LpAPLp remains nearly constant while, LpAP reaches a critically low concentration, L remains at its maximum, A and P reach peak free concentrations, after which Lp begins to accumulate rapidly. The system transitions to rapid reformation of LpA and subsequent LpAK formation, leading to the cycle reset.

The cycle reset and transition to the next oscillation involve rapid Lp accumulation as LpAK catalytic activity outpaces LpAP's ability to consume Lp. Accumulated Lp binds with free A to form LpA, whose

concentration increases rapidly. LpA then binds with K to form LpAK, further accelerating Lp production. Free L is rapidly converted to Lp by increasing LpAK activity, decreasing L concentration. Finally, high concentrations of Lp, LpA, and LpAK are restored, L concentration reaches its minimum, and the system returns to the initial state of Phase 1.

Version 2

The lipid oscillator model exhibits a biphasic cycle, with each phase characterized by distinct dynamics and molecular interactions. Phase 1 initiates with high concentrations of Lp, LpP, LpA, and LpAK, while L, LpAP, and LpAPLp are present at low levels. The primary process during this phase is the conversion of Lp to L, catalyzed by LpAP. As free Lp depletes, LpA dissociates into Lp and A, destabilizing both LpAK and LpAP. A critical structural asymmetry in the reaction network favors LpAP formation: the dissociation of membrane-localized complexes releases free Lp, which stabilizes LpAP but not LpAK. This asymmetry confers a fundamental advantage to phosphatase activity, ensuring the eventual depletion of free Lp regardless of specific parameter values. Phase 1 concludes with the exhaustion of free Lp, low concentrations of LpA, LpP, and LpAK, and a peak in LpAPLp concentration. The transition to Phase 2 is marked by a dramatic shift in system dynamics. The depletion of Lp precludes LpAPLp formation, leading to rapid accumulation of free L and LpAP. LpAKL concentration decreases as its free form destabilizes and dissociates. The remainder of Phase 2 is characterized by LpAP depletion and the accumulation of membrane-complex components. The system experiences net delocalization and decomplexation as LpAP steadily dissociates into LpA and P, with LpA further dissociating into Lp and A. Any Lp released is immediately bound and catalyzed by the remaining LpAP. Throughout this phase, L concentration approaches its maximum, with nearly all lipid present as free L, while free A and P concentrations rise. K remains largely unbound due to substrate scarcity. Several key mechanisms govern Phase 2. LpAP acts as the primary inhibitor, efficiently binding Lp released from LpAP/LpA dissociation even at low concentrations. This prevents net formation of LpA or LpAK until LpAP is sufficiently depleted. A zero-

order kinetics window emerges as the remaining LpAP becomes saturated, allowing transient Lp accumulation without a proportional increase in consumption. The catalytic balance is crucial, with LpAPLp turnover rate needing to be high enough to prevent Lp release from resaturating LpAP. This suggests a constraint on LpAPLp catalytic efficiency and LpAP unbinding rate. LpAP maintains a competitive advantage by outcompeting A and P in binding the small amounts of Lp released, key to sustaining its inhibitory effect. The critical transition concluding Phase 2 involves transient Lp accumulation as LpAP reaches its minimum, protected by the zero-order kinetics of saturated LpAP. Accumulated Lp binds to free A, forming LpA, which can then associate with either K or P. Even if LpAP formation is initially favored, LpAK can initiate positive feedback under specific conditions. This requires LpAK to possess higher catalytic efficiency, faster product release, higher turnover number, greater stability, and access to higher substrate concentration compared to LpAP. If these conditions are met, LpAK can generate Lp faster than LpA or LpAP can consume it, establishing a positive feedback loop that rapidly resets the cycle. As Phase 2 concludes, LpAPLp remains nearly constant, LpAP reaches a critically low concentration, L remains at its maximum, and A and P reach peak free concentrations. Subsequently, Lp begins to accumulate rapidly, leading to the reformation of LpA and LpAK, thus resetting the cycle. The cycle reset is characterized by rapid Lp accumulation as LpAK catalytic activity surpasses LpAP's consumption capacity. This accumulated Lp swiftly binds with free A to form LpA, which then associates with K to form LpAK, further accelerating Lp production. Concurrently, free L is rapidly converted to Lp by the increasing LpAK activity. The cycle completes as high concentrations of Lp, LpA, and LpAK are restored, L concentration reaches its minimum, and the system returns to the initial state of Phase 1.

Version 3

1. Lp Spike (Positive Feedback Loop)

The oscillation cycle begins with a rapid increase in the concentration of phosphorylated lipid (Lp), known as the Lp spike. This spike is characterized by a positive feedback loop that drives the rapid generation of Lp. As Lp is produced, it binds to either the adaptor protein (A) or the phosphatase (P), leading to similar spikes in the concentrations of LpP, LpA, LpAK, and LpAP complexes.

The positive feedback loop operates through the following mechanism: Initially produced Lp binds to A, forming LpA. This LpA then associates with the kinase (K) to form LpAK. The LpAK complex catalyzes the production of more Lp from L, further fueling the cycle. This self-reinforcing process drives the rapid increase in Lp concentration.

However, this rapid increase doesn't continue indefinitely. The Lp spike reaches its peak when the production of LpAP catches up with the production of Lp. At this point, LpAP begins to convert Lp back to L at a rate faster than LpAK can produce Lp. Interestingly, the concentration of LpAK itself peaks before the Lp concentration does. This LpAK peak sets the stage for the reversal of the Lp spike, as it marks the point where LpAK can no longer fuel its own production via the positive feedback loop.

When examining the individual reaction rates during this phase, a specific sequence emerges. The LpAP formation rate peaks first, followed by the LpA formation rate, and finally the LpAK formation rate. An intriguing observation is that both the LpA and LpAK formation rates show a smaller subsequent peak shortly after their main peak. The reason for this secondary peak is not yet fully understood and warrants further investigation.

2. Phase 1

Following the Lp spike, the system enters Phase 1, which is characterized by a dramatic drop in free Lp concentration to near zero. During this phase, membrane-bound species either disassociate or convert to LpAP.

One of the key processes during Phase 1 is the progression of LpP. The concentration of LpP decreases to zero as it is converted into free L. Correspondingly, the concentration of free L rises as LpP is depleted. This conversion represents a shift in the balance of lipid species from the phosphorylated to the unphosphorylated form.

An important characteristic of this phase is the lack of new net LpA creation from the remaining Lp. This is due to two factors: first, the low amount of free A available in the system, and second, the dominance of the membrane-localized phosphatase in binding any Lp that becomes available. This dynamic illustrates a general pattern in the system: net production of membrane-bound complexes, which occurs via Lp binding to A, can only happen in the absence of LpAP. When LpAP is present, it efficiently binds all available Lp, preventing the formation of other Lp-containing complexes.

The behavior of free species during this phase is complex. The concentration of free A remains nearly constant, while the concentrations of free LpA and free LpAK fall. Simultaneously, the concentration of LpAPLp rises. The falling concentration of LpP during this time indicates that free LpA and LpA produced from LpAK dissociation is directly binding to free P as it turns over its ligand. This process must wait for LpP to catalyze and return to unbound P before forming more LpAP/LpAPLp.

A crucial aspect of Phase 1 is the difference in saturation between LpAP and LpAK. LpAP remains completely saturated throughout this phase, meaning it's entirely bound in the form of LpAPLp. Even as new LpAP is created, it binds so strongly to the remaining free Lp that all of it is found in its enzyme intermediate form. In contrast, LpAK remains far from saturation during this phase. This is due to its faster turnover rate and lower binding affinity for L, even as the concentration of L is increasing. As a result, the concentration of LpAKL remains constant (the decrease in free LpAK is roughly offset by the increase in L), while LpAK decreases steadily as it dissociates into free K and LpA.

3. Interphase Transition

The transition between Phase 1 and Phase 2 is marked by several significant events. This interphase transition is characterized by the depletion of free Lp and the maximal concentration of LpAPLp. It represents a critical point in the oscillation cycle where the system shifts from one dominant state to another.

During this transition, the concentrations of LpA, LpAK, LpAKL, and LpP all drop to near zero, although this decrease occurs more slowly than the depletion of free Lp. Simultaneously, there is a rapid rise in the concentration of LpAP. This increase in LpAP occurs because there is no more free Lp available to keep LpAP bound in the form of LpAPLp, leading to a rapid desaturation of the enzyme.

The behavior of free species during this transition is particularly interesting. The concentrations of free P and free A rise rapidly immediately prior to this transition point. However, their rate of increase slows down slightly at the point where LpP and LpAK effectively reach zero concentration. This creates a slight kink in the time series of free P and A, representing a regime change. Initially, these free species are produced as decay products of LpA, LpAK, LpP, and LpAP. However, as the system moves into Phase 2, they are primarily produced from the decay of LpAP alone.

The concentration of free L exhibits a similar behavior to free P and A. It rises sharply as the system approaches the transition point but then slows down abruptly. This change in behavior occurs because free L is no longer being produced by the easy conversion of free Lp. Instead, its growth becomes dependent on the cannibalistic behavior of LpAP during Phase 2, where LpAP decays and the remaining LpAP binds to the free Lp decay product, converting it to free L.

4. Phase 2

Phase 2 is the simplest phase of the oscillation cycle in terms of its dynamics. It is dominated by the decay of LpAP until the system reaches a critical threshold that triggers the next Lp spike.

During this phase, the concentrations of free P and free A continue to rise as a direct result of LpAP decay. Meanwhile, the concentration of free L continues to rise slowly, approaching its maximum where all lipid in the system is in the form of free L, with no Lp or membrane-bound complexes present.

An interesting feature of this phase is the behavior of LpAPLp. Despite the ongoing decay of LpAP, the concentration of LpAPLp remains roughly constant. This stability is due to a balance between two opposing processes: the decay of LpAP produces extra Lp substrate, but it also equally removes enzyme from the system. These effects cancel each other out, resulting in a relatively stable LpAPLp concentration.

As Phase 2 progresses, the concentration of LpAP continues to decrease. Eventually, it reaches a critical threshold at which it's no longer able to bind the basal level of Lp being generated by free K. This marks the beginning of the transition to the next Lp spike.

5. Transition to Lp Spike (Cycle Restart)

The transition from Phase 2 back to the Lp spike represents the completion of one oscillation cycle and the beginning of the next. This transition occurs when LpAP reaches a critical threshold concentration below which it can no longer effectively bind all the Lp being produced in the system.

At this point, the small amount of Lp being continuously generated by free K begins to accumulate. This excess Lp becomes available to bind with free A, forming LpA. The newly formed LpA can then bind with K to form LpAK, which in turn catalyzes the production of more Lp.

This sequence of events reactivates the positive feedback loop that characterizes the Lp spike. As more Lp is produced, it fuels the formation of more LpA and LpAK, which in turn produce even more Lp. This cascading effect rapidly increases the concentration of Lp, triggering the next Lp spike and restarting the oscillation cycle.

The transition point is crucial for the maintenance of oscillations in the system. It represents the moment when the inhibitory effect of LpAP is overcome, allowing the activating kinase pathway to dominate once again. The precise timing and dynamics of this transition are likely key determinants of the oscillation period and amplitude.

Effects of Adaptor protein mediated localization

The lipid-phosphorylation oscillator model exhibits complex dynamics that are critically dependent on the behavior of the intermediate species LpA. Our analysis reveals that LpA plays a multifaceted role in maintaining robust oscillations, acting as a key mediator of information transfer within the system. The stability of LpA emerges as a crucial factor in determining the system's oscillatory behavior. Our observations indicate that the system exhibits greater robustness to LpA instability compared to high stability. This counterintuitive finding can be explained by considering LpA's function as a shared intermediate between the kinase and phosphatase pathways.

There exists an optimal range of LpA stability that balances the need for efficient complex formation with the requirement for rapid redistribution of Lp between pathways. Excessive stability of LpA can lead to several detrimental effects. First, it can result in sequestration of Lp, reducing the pool available for driving phase transitions. Second, it can increase cross-talk between oscillation phases due to simultaneous potentiation of both enzymes. Third, it can cause slower response to changing conditions, potentially disrupting the timing of phase transitions.

Unlike other components in the network that follow a more unidirectional flow, LpA must alternate between associating with kinase and phosphatase. High stability can hinder this necessary flexibility, impeding the system's ability to transition between phases. From an information theory perspective, overly stable LpA can be conceptualized as introducing noise into the system, reducing the fidelity of the

signal that drives oscillatory behavior. This perspective aligns with the observation that the system favors conditions allowing for more discrete signaling between different parts of the network at different times.

The timescales of LpA formation and dissociation relative to other processes in the system play a crucial role in maintaining robust oscillations. Our analysis suggests that increasing both formation and dissociation rates of LpA improves the sharpness and synchrony of oscillations.

LpA functions as a crucial information transducer in the system. Fast LpA kinetics allow for rapid assessment of the system state, quick equilibration enabling swift responses to changes in Lp, K, and P concentrations, and maintenance of phase coherence across the system. Interestingly, oscillation integrity does not require significant LpA mediation. Instead, LpA's role appears to be more about facilitating quick state transitions rather than actively controlling the oscillatory behavior.

Fast LpA kinetics allow for high fidelity of feedback, enabling quicker system responses to changes in Lp levels, reduced lag between the system state and enzyme complex formation, and more efficient operation of feedback loops, potentially sharpening transitions between phases.

Kinetic asymmetry between kinase and phosphatase pathways is necessary for oscillations

The higher catalytic rate of the kinase ($$k_{cat}^{LK}$$) contributes significantly to the system's oscillatory behavior through several mechanisms. Primarily, it allows for rapid production of Lp once the kinase pathway is activated, which is crucial for the sharp transition from Phase 2 to Phase 1 of the oscillation cycle. As Lp is produced, it fuels the formation of more LpAK complexes, which in turn produce more Lp. This positive feedback loop is a key driver of the Lp spike that characterizes the beginning of each cycle. The higher $$k_{cat}^{LK}$$ enhances the efficiency of this feedback mechanism, allowing for a rapid accumulation of Lp even when the initial concentration of LpAK complexes is low.

Moreover, the higher $$k_{cat}^{LK}$$ plays a critical role in overcoming the initial phosphatase dominance at the end of Phase 2, when the unphosphorylated lipid L is abundant. This rapid shift in dominance is essential for initiating the transition to Phase 1 and maintaining the oscillatory behavior of the system. The high catalytic rate allows the kinase pathway to quickly become dominant, even when starting from a state where the phosphatase pathway has been prevailing. This ability to rapidly switch the system's state is a key feature of many biological oscillators, allowing for clear demarcation between different phases of the cycle.

Additionally, the higher $$k_{cat}^{LK}$$ makes the system more responsive to small increases in Lp concentration. This sensitivity enhances the switch-like behavior of the system, allowing for sharp transitions between phases. Even a small accumulation of Lp can trigger a rapid cascade of Lp production, driving the system into Phase 1. This sensitivity to small changes is crucial for the robustness of the oscillations, as it allows the system to reliably transition between phases even in the presence of small fluctuations or perturbations.

While the catalytic rate favors the kinase pathway, the binding affinity favors the phosphatase pathway ($$k_f^{LK} < k_f^{LP}$$). This asymmetry in binding affinities contributes to the system's behavior in several important ways. The lower binding rate ($$k_f^{LK}$$) for the kinase pathway means that it doesn't activate too easily. This delayed activation is crucial for preventing premature termination of Phase 2, ensuring that the system spends sufficient time in the L-dominated state before transitioning to the Lp-dominated state. This delay allows for the accumulation of L and other necessary components, setting the stage for the next oscillation cycle.

Conversely, the higher binding rate ($$k_f^{LP}$$) of the phosphatase pathway allows it to quickly respond to Lp production. This rapid response provides a counterbalance to the kinase pathway, acting as a "brake" on the system. It helps prevent runaway Lp production and contributes to the system's ability to maintain stable oscillations. The phosphatase pathway's ability to quickly bind and process Lp ensures

that the Lp-dominated state doesn't persist indefinitely, allowing for the eventual transition back to the L-dominated state.

The combination of lower binding but higher catalysis for the kinase pathway creates a threshold effect that must be overcome to initiate Phase 1. This threshold effect is crucial for the switch-like behavior of the system. It ensures that the transition to Phase 1 only occurs when sufficient Lp has accumulated to overcome the phosphatase's buffering capacity. This creates a distinct threshold where the kinase pathway suddenly becomes dominant, leading to a sharp transition to Phase 1.

These asymmetries in catalytic rates and binding affinities create several synergistic effects that enhance the robustness and efficiency of the oscillator. They help create distinct phases within the oscillation cycle, with Phase 2 dominated by phosphatase binding due to its higher binding affinity, while Phase 1 is driven by kinase catalysis due to its higher catalytic rate. This clear delineation of phases contributes to the stability and regularity of the oscillations.

The switch from phosphatase dominance (due to higher $$k_f^{LP}$$) to kinase dominance (due to higher $$k_{cat}^{LK}$$) can be quite sharp. This sharp transition is a key feature of many biological oscillators, allowing for clear demarcation between different states of the system. During Phase 2, small amounts of Lp produced are quickly bound by the phosphatase due to its high binding rate ($$k_f^{LP}$$). This rapid binding prevents premature activation of the kinase pathway, making the system robust against small fluctuations in Lp concentration.

Furthermore, during Phase 1, while the phosphatase might bind Lp more quickly due to its higher binding rate, the higher catalytic rate of the kinase ($$k_{cat}^{LK}$$) ensures efficient conversion of L back to Lp. This efficient use of substrates helps maintain the oscillatory behavior of the system. The rapid Lp production outpaces the phosphatase activity, maintaining the Lp-dominant state until substrate depletion or other factors lead to the eventual transition back to Phase 2.

Dimensional reduction is necessary to augment the kinetic asymmetry at the right times

The dimensionality factor (DF) in our model represents the effect of membrane localization on reaction rates, specifically by increasing the forward binding rate constants for reactions that occur on the membrane surface. Our analysis reveals that DF plays a crucial role in enhancing the robustness of the lipid oscillator system, particularly with respect to the necessary differences between the kinase and phosphatase pathways. Higher DF values allow these differences to be less finely tuned while still maintaining robust oscillatory behavior, thus expanding the range of conditions under which the system can function effectively.

The primary mechanism by which DF enhances system robustness is through the amplification of intrinsic differences between the kinase and phosphatase pathways. This amplification is based on how DF affects reaction rates differently depending on the availability of substrates. For instance, at the end of Phase 2, when unphosphorylated lipid (L) is abundant, DF strongly amplifies the reaction where the kinase binds to L. This enhancement of the kinase pathway's ability to initiate a phase transition compensates for potentially suboptimal inherent reaction rates.

We can understand this amplification by considering how DF affects the effective reaction rates. For both the kinase and phosphatase pathways, DF increases their binding rates to their respective substrates. However, the impact of this increase is not the same for both pathways due to the different amounts of substrates available during various phases of the oscillation cycle.

While DF increases both the kinase and phosphatase binding rates by the same factor, the absolute difference between these rates becomes larger as DF increases. This growing difference becomes significant when we consider the actual reaction rates, which depend on both how quickly the enzymes can bind (affected by DF) and how much substrate is available.

During Phase 2, when L is abundant, the kinase reaction rate benefits more from the DF increase than the phosphatase reaction rate. This is because there's more L available for the kinase to act on compared to

the amount of Lp available for the phosphatase. This differential amplification allows the system to maintain sharp transitions between phases even when the inherent reaction rates are less optimally tuned.

For example, in situations where the kinase's inherent binding rate is lower than ideal, higher DF values can compensate by increasing the effective binding rate of the kinase pathway when L is abundant. We can think of this as DF lowering the bar for what counts as a "good enough" kinase binding rate to maintain oscillations.

Furthermore, DF enhances the system's ability to amplify weak signals. Small increases in Lp concentration at the end of Phase 2 are magnified by DF. This ensures that the kinase pathway can overcome the phosphatase's inhibitory effect and initiate Phase 1, even when the inherent differences between the pathways are less pronounced. We can think of this as DF making the system more sensitive to small changes, allowing it to switch phases more easily.

The impact of DF on system robustness is further evidenced by its ability to maintain oscillations across a wider range of conditions. Our analysis shows that increasing DF allows the system to tolerate greater variations in reaction rates while still producing stable oscillations. We can visualize this as DF expanding the "sweet spot" of conditions where oscillations occur, making it easier for the system to find and maintain a working rhythm.

It's important to note that DF's influence on system behavior is not the same across all phases of the oscillation cycle. The impact of DF shifts dynamically based on changing substrate concentrations. For instance, in Phase 1 when Lp is abundant, DF amplifies the reaction where the phosphatase binds to Lp, enhancing the phosphatase pathway's ability to eventually terminate Phase 1. This dynamic shifting of dominance contributes to the overall robustness of the oscillatory behavior by ensuring that neither pathway remains dominant indefinitely.

***Reminder* Except when we are showing examples of what the oscillations look like (in which case we plot concentrations vs time), in general all of our plots are going to have a parameter, or product of parameters on the x-axis. Like DF, or kcatLP/kcatLK, or A/L, etc. The y-axis will be a useful observable, such as whether solutions exist for those parameters, how many solutions exist, or what the period is, or the amplitude.**

NOTES on PARAMETER REGIMES for Concentrations: Typically we will want the concentration of L to be higher than A. Otherwise, if A>>L, then it is impossible for a large fraction of A to transition to the membrane, because it must have enough binding sites. So we can argue that we are generally interested in regimes where we can get relatively large amplitude oscillations as measured by A going on and off the membrane, and therefore we will have L>A. In real systems, enzymes have much lower concentrations than A, and it would likely be more energy efficient if we could have large amplitude oscillations with small numbers of enzymes, so if A>K in particular is true, and yet we can get large amplitudes, that should be more efficient than the same size oscillations with K>A (because I'm assuming there would be more L->Lp conversions in the latter). K is the one that consumes ATP. Phosphatases use hydrolysis to break bonds.

3.0 Oscillations can be found for experimentally defined parameter regimes:

Reaction	**Source**	$k_{on}\ (\mu M^{-1}\ s^{-1})$	$k_{off}\ (s^{-1})$	$K_d\ or\ K_M\ (\mu M)$	$k_{cat}\ (s^{-1})$
Binding of PIP2 to AP2	Honing et al., 2005	0.7×10^{-3}	2.0×10^{-3}		
Binding of AP2 Subunit to PIP5K	Krauss et al., 2006	0.118	0.609		
Binding of Synaptojanin 1 to AP2 α-Appendage	Praefcke et al. 2004			29	
Catalytic Activity of Synaptojanin 1 on PIP2	Paesmans et al., 2020			39	85.3

Catalytic Activity of PIP5K1C	Shulga et al., 2012			15	

Table 1: Experimental Values. In simulations, the value of kcat for PIP5K was determined using the formula kcat = (KM × kon)– koff , where kon and koff were sampled from a range of physically realistic values that did not lead to a negative catalytic rate constant. Similarly, kon for Synaptojanin 1 was sampled from physically realistic ranges, and koff was calculated via koff = (KM × kon)– kcat. kon for the binding of Synaptojanin to AP2 was also sampled from physically realistic ranges, and koff was calculated using koff = kon × Kd. McIntire et al. report different values for the catalytic activity of Synaptojanin 1 on PIP2 (KM = 138.5 μM, kcat= 50. s-1), though these were not used in our investigation (2013).

Commented [EG43]: These will need explainers. I see the concentration of the long periods for the KmLK<KmLP which is good but otherwise I don't get the green/what else you're trying to show

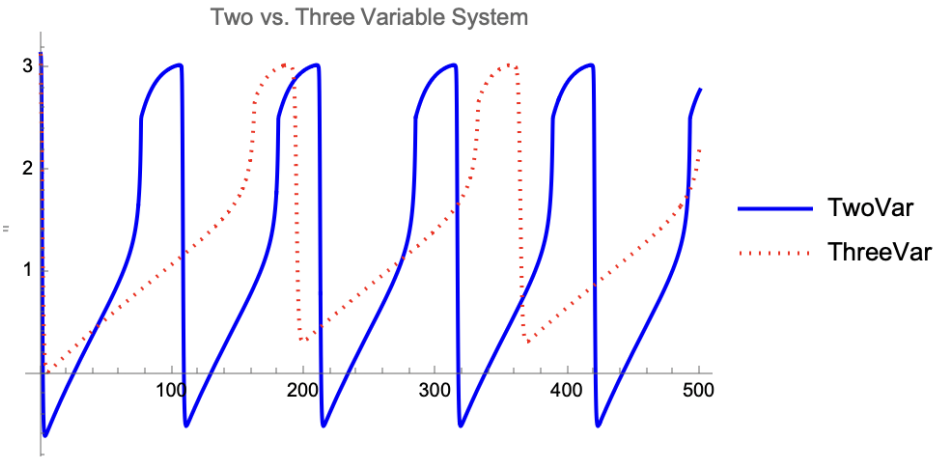

Model reduction to two variables demonstrates oscillations in L and Lp are retained. Poincare Bendixson can be applied to this model to prove that it oscillates, as long as a single fixed point

exists, is bounded, and the trace of the Jacobian at that fixed point has parameter regimes where it is positive.

It might be helpful at this point to set the K+L and P+Lp backward rates to 0, because kcat is typically faster than this unbinding reaction.

At this point, if we simplify the model by, for example, eliminating dimensional reduction in one of the enzymes, set the binding of the enzyme to A to zero. So kfAP=0, eliminates dimensional reduction for the phosphatase P. kfAK=0 eliminates dimensional reduction in the kinase K. If both are zero, we expect no oscillations. This is almost the same as setting DF=1, except that the AP and AK species can't form. If [A]total=0, one can prove no oscillations.

3.5 Reaction model is not structurally attractive

We conducted a detailed stability analysis of our biochemical reaction network using the LEARN software package. The network consists of 16 species and 44 reactions, with a stoichiometric space of 12 dimensions, reflecting the presence of 4 conserved quantities that reduce the effective dimensionality by 4. Show derivation in SI methods

The analysis confirmed that the network has a positive vector in the kernel of the stoichiometry matrix, indicating the potential existence of positive steady states. This suggests that there are feasible combinations of species concentrations that can maintain dynamic equilibrium.

The network's structural persistence is evidenced by the absence of critical siphons, ensuring that no species can be entirely depleted. This property supports the robustness of the network's dynamics.

The LEARN package evaluated several necessary conditions to determine the feasibility of constructing a Robust Lyapunov Function (RLF) for our network:

1. **Critical Siphon Necessary Condition**: This condition is satisfied, confirming that the network lacks critical siphons and that all species are maintained.
2. **Sign Pattern Necessary Condition**: This condition is satisfied, indicating that the Jacobian matrix entries have consistent signs, which supports the monotonicity of reaction rates.
3. **P Matrix Necessary Condition**: This condition is violated. The P matrix condition is essential for the existence of a piecewise linear RLF (PWL RLF), and its violation means that such a function cannot be constructed for our network.

The violation of the P matrix necessary condition indicates that our network is not structurally attractive. Structural attractiveness in biochemical reaction networks ensures global stability through the existence of a universal Lyapunov function, independent of specific kinetic parameters. Structurally attractive networks are robust to variations in kinetic parameters and environmental conditions, guaranteeing consistent behavior.

Given that the network is known to exhibit oscillatory behavior for certain parameter values, the lack of structural attractiveness is significant. It suggests that the network's dynamics can include multiple steady states, oscillations, or even chaotic behavior, depending on the parameter regime. This complexity arises from the network's failure to meet the stringent P matrix condition, which is critical for constructing a PWL RLF. Without this function, we cannot guarantee that the network will consistently converge to a single steady state.

Commented [EG44]: Are you sure this is true? I would have to read the paper more closely, but I thought the violation of this condition solely means that there is not a Liapunov function of the PWL RLF form, but there could be another Liapunov function (it is sufficient but not necessary)

Commented [EG45]: Haven't we observed this though ourselves? Not sure it is necessary to bring this up

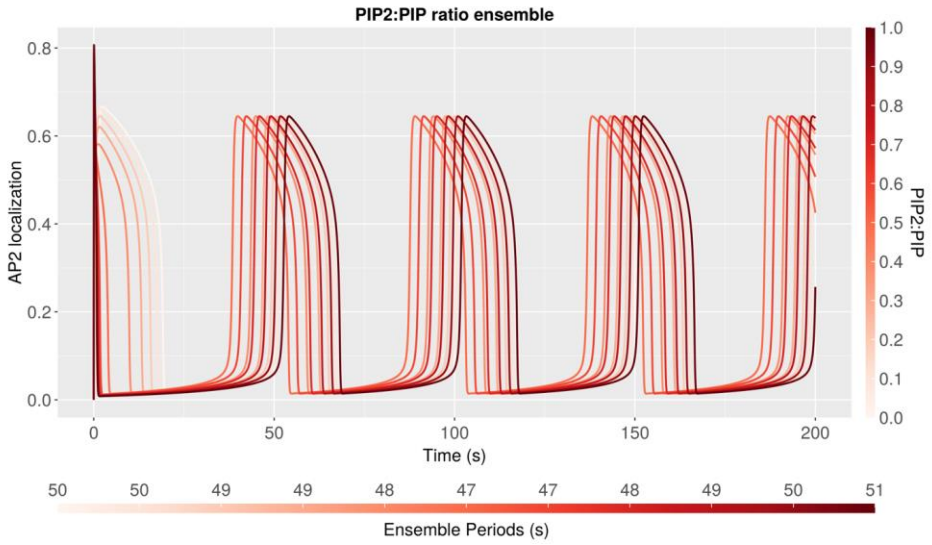

Oscillation period is invariant to initial ratio of PIP:PIP2*. Trajectories solved for ratios from 0.1 to 1.0, while fixing total lipid mass, converge to same period and limit cycle, but phase shifted. Altered PIP:PIP2 simply changes the starting position on the invariant manifold defined by the relative abundances of lipid, adaptor, and enzyme.*

Internal transients starting from different initial proportion of PIP:PIP2 (while total lipid is conserved), show a phase shift before convergence onto a limit cycle.

3.2 Larger dimensionality factors favor oscillations at intermediate K_D^{LA} values

- Probably not important, perhaps superseded by mechanistic interpretability
- Mechanism of oscillation no longer needed to be explained from population analysis
- Instead, this section is here to:

- Provide visual of viable solution space. Sparsity, shape of oscillatory solutions compared to surrounding volume.
- Effect of DF at a population level, similar to figure below, hopefully being able demonstrate the necessity of DF and how it shapes/expands viable solution space. In other words, how DF effects robustness using solution space as a measure.
- Experimental systems will have distribution of initial conditions, confidence intervals around any measured parameter values; population analysis is appropriate to approximate this.

In our exploration of the biochemical oscillator model, we systematically varied the dimensionality factor (DF) and the lipid-adaptor dissociation constant $\boldsymbol{K_D^{LA}}$. Our analysis focused on understanding how these parameters influence the oscillatory dynamics of the system. The oscillation period, represented by a color gradient from green (shorter periods) to yellow (longer periods), served as the key indicator of dynamical behavior.

Our findings reveal a distinct correlation between DF and the oscillation period across a spectrum of $\boldsymbol{K_D^{LA}}$ values. Notably, as DF increased, a trend toward shorter oscillation periods was observed, particularly pronounced at intermediate $\boldsymbol{K_D^{LA}}$ values (approximately 10^{-1} to 10^{0} μM). This region highlighted a 'sweet spot', where the period sensitivity to changes in DF was at its peak, suggesting that DF most effectively enhances catalytic interactions when the A-L complex exhibits a balanced stability—not too transient, yet not overly stable.

At mid-range $\boldsymbol{K_D^{LA}}$ values, the oscillation period displayed high sensitivity to variations in DF, indicating a dynamic response where the balance between free and membrane-bound enzyme states critically influences the system's temporal behavior. Conversely, at the extremities of $\boldsymbol{K_D^{LA}}$ values—both very low

and very high—the modulation of enzyme kinetics by changes in DF was considerably less pronounced. In scenarios of high complex stability (low $\boldsymbol{K_D^{LA}}$), the modulation becomes less impactful due to a ceiling effect, where enzymatic activity is already maximized. In contrast, at high $\boldsymbol{K_D^{LA}}$ values, the instability of the complex limits the effective modulation by DF, diminishing its impact on oscillatory dynamics.

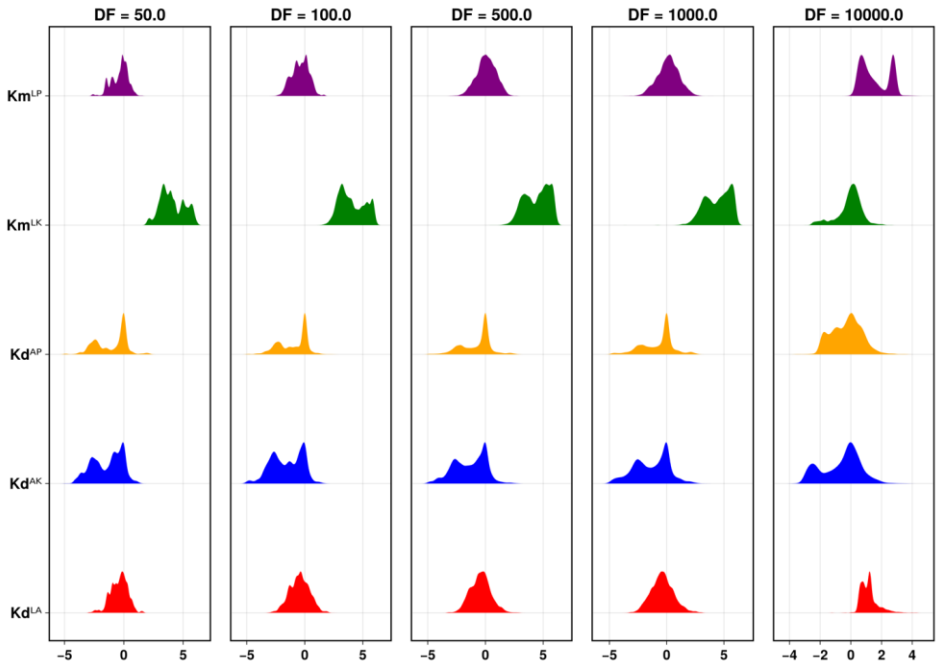

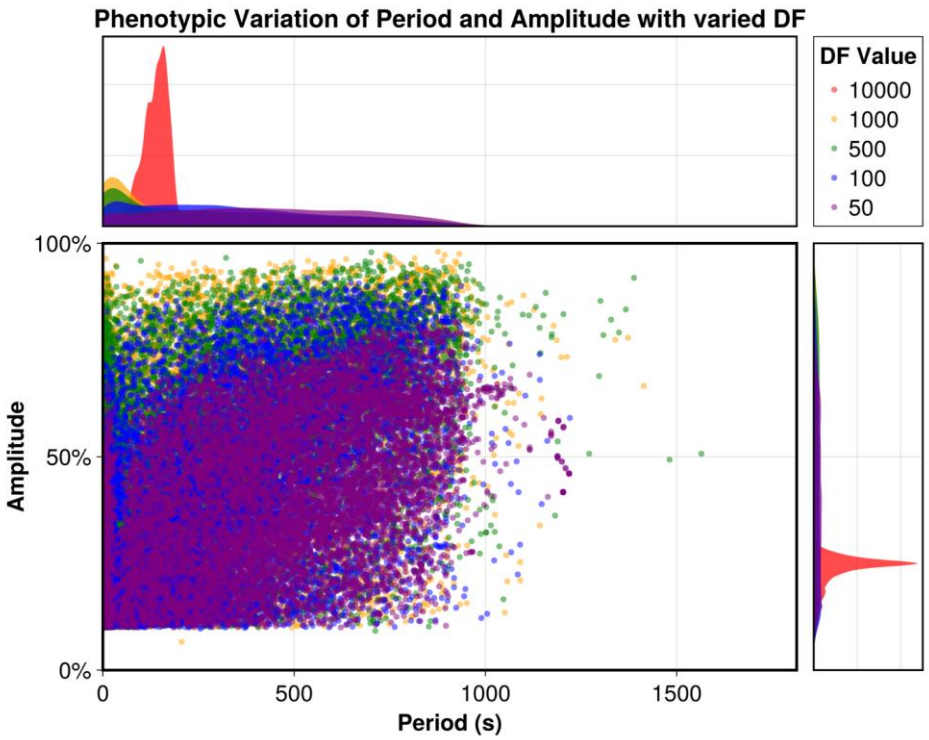
Phenotypic Variation of Period and Amplitude with varied DF
DF Value
10000
1000
500
100
50
100%
50%
0%
Amplitude
0
500
1000
1500
Period (s)

3.3 Oscillation period can be smoothly tuned via scaling DF

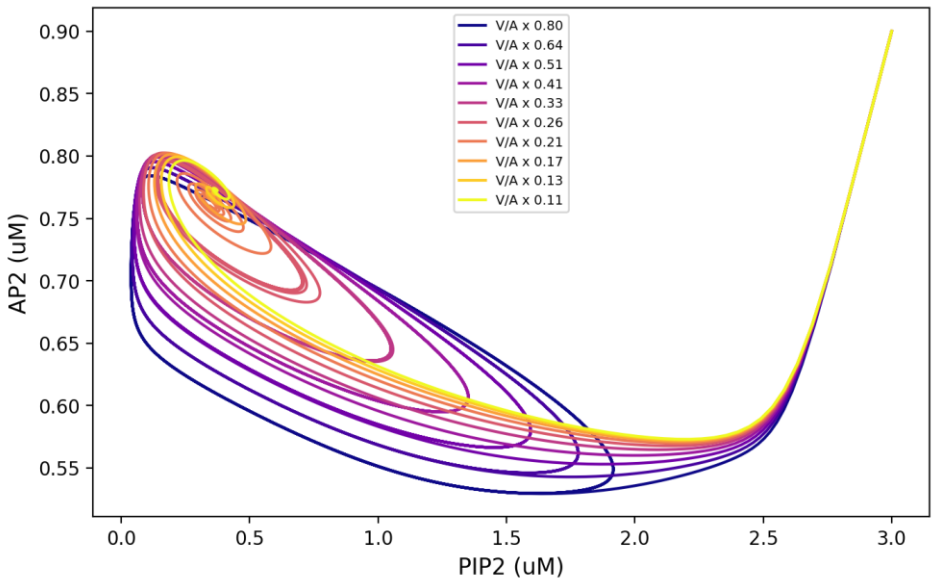

Period tunability is defined as the change in period with respect to a tuning parameter divided by the change in amplitude (of some variable) with respect to that same parameter. In other words, it is the degree by which the period of an oscillator can be changed independent of the amplitude. In positive-negative feedback oscillators, which are called hysteresis-driven oscillators, the positive feedback creates bistability between two steady states, with the system walking about a hysteresis loop between those two states, and the speed of that walk determined by the reaction velocities. This means that for a hysteresis oscillator where those steady states are primarily determined by a subset of the reaction systems (with peripheral reactions having no affect due to symmetries in the reaction network, conservation laws), those peripheral reaction kinetics can be used as tuning parameters to independently control the speed of the walk between the steady states, i.e. the period is tunable.

With the mode of oscillation described in the prior subsection, we observe high amounts of period tunability of the lipid composition ratio with respect to multiple kinetic parameters, most notably DF. Increasing DF reduces the period of oscillations without affecting the maximal saturation or depletion of the lipid species. We hypothesize that this is because the period of the oscillator is primarily determined by the amount of time it takes for

3.4 Self-assembly can be synchronized with oscillatory membrane dynamics

Commented [MJ46]: Change to histogram

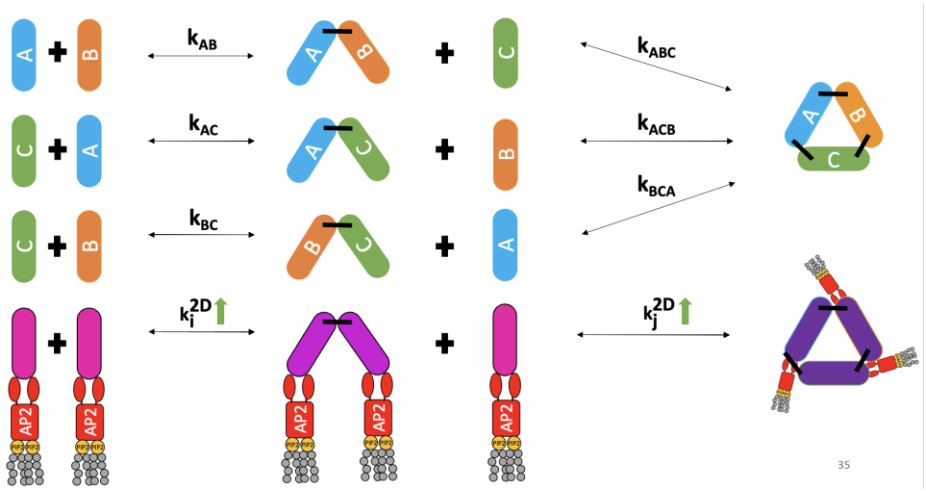

Figure 5. Illustration of the extended self-assembly process involving the trimerization of three heteromers (A, B, and C) with the incorporation of a lipid membrane binding interface mediated by the adaptor protein AP2. This figure depicts the sequential binding interactions leading to the formation of various heteromer complexes, both in solution and membrane-bound forms. The rate constants denote the reaction rates for the formation and dissociation of these complexes. The incorporation of AP2 and its interaction with the lipid membrane is represented by the 2D rate constants This modified self-assembly mechanism was designed to test the applications and composability of a biological oscillator in driving periodic dynamics in non-periodic systems. The right side of the figure demonstrates the fully assembled trimer complexes, highlighting the role of the lipid membrane in facilitating these interactions.

3.5 Oscillatory solutions can be recapitulated with stochastic simulation algorithms

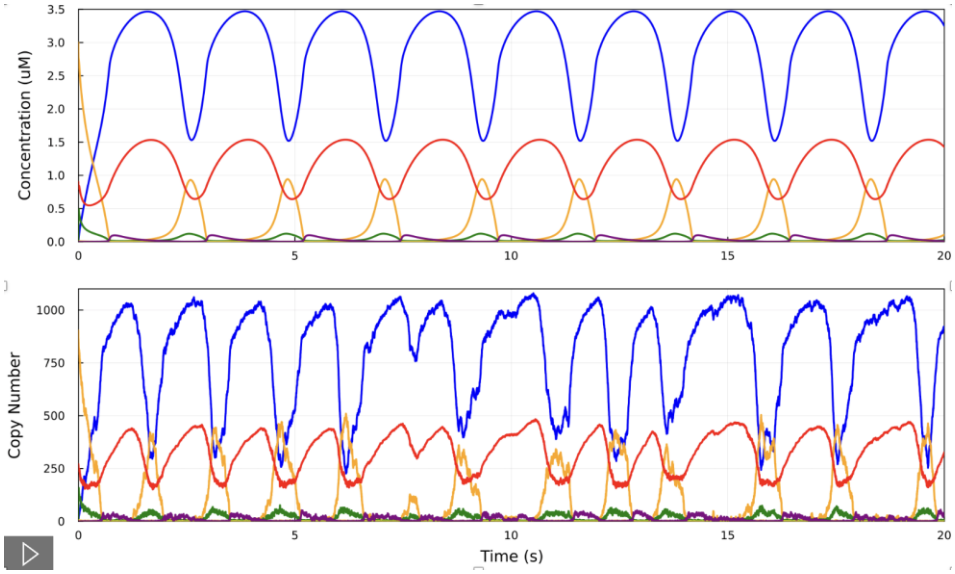

3.6 Oscillatory solutions can be recapitulated in spatially resolved reaction-diffusion simulation (NERDSS)

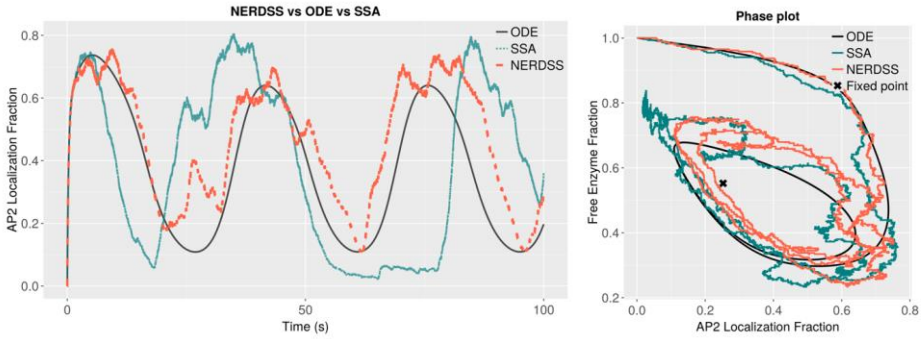

The rate limiting step must be first order, such as the unbinding or catalytic rate constants with units of s^{-1}, to ensure NERDSS matches deterministic simulation. This logic follows that of previous research modeling temperature sensitivity in biological oscillators, while also compensating for diffusion by

ensuring the period determining steps aren't dependent on spatial dynamics that violate the mass action assumptions of our ODE model.

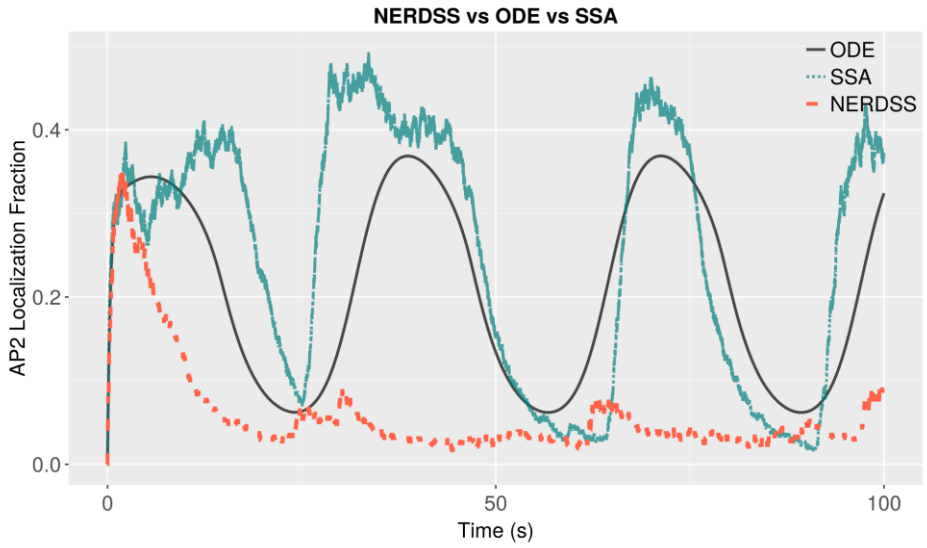

***SSA fails to predict NERDSS**. This discrepancy represents spatial constraints that limit the apparent viable solution space as computed by the non-spatial simulations.*

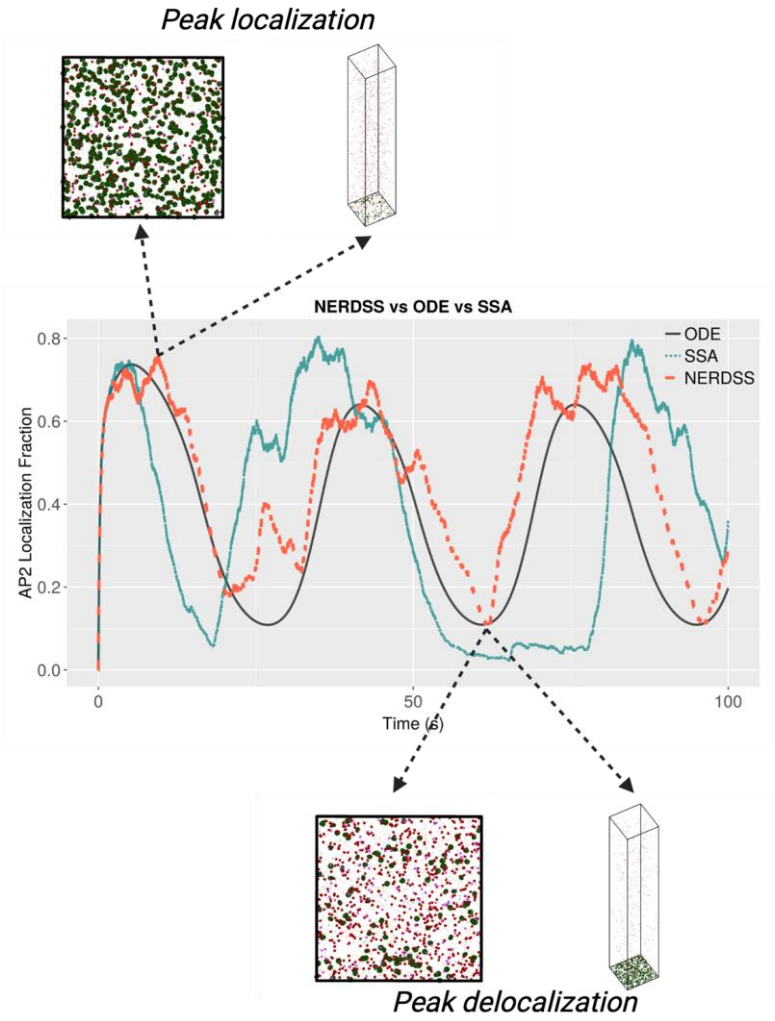

DISCUSSION

In this study, we presented a minimal general model for a biochemical oscillator driven by dynamically tuned membrane localization, inspired by the process of clathrin-mediated endocytosis (CME). Our model exploited the mechanism of membrane localization to produce oscillations, with the frequency of the

oscillations tunable by the volume to surface area (V/A) ratio. This tunability allows for direct control of the oscillator's period through mechanical intervention, without the need for engineering the underlying biochemistry.

By comparing our model with other biochemical oscillators, we highlighted its advantages, such as its robustness to noise, flexibility in tunability, and potential applications in timed drug delivery and real-time monitoring of cell growth or shape change. The results of our analyses demonstrated the oscillator's performance in various parameter regimes, sensitivity to key parameters and initial conditions, and its behavior in both spatial and non-spatial contexts.

Despite the promising findings, several outstanding questions and areas for further exploration remain. First, experimental validation of the proposed model is crucial. It would be interesting to test the model in vivo, employing synthetic biology techniques to construct the oscillator system and validate the predicted behavior in a controlled environment.

Second, a more detailed investigation of the role of specific reaction mechanisms and parameters is necessary to understand the oscillator's behavior better. This could involve a deeper exploration of the model's robustness under different conditions or the inclusion of additional layers of regulation and feedback to study their impact on the system's performance.

Third, expanding the model to incorporate other cellular processes, such as self-assembly or bioluminescence, could help investigate potential applications in biosensing, drug delivery, and monitoring of cell growth or shape change. By coupling these processes to the oscillator through an adaptor binding interface, a wide range of possibilities for synthetic biology applications could be explored.

In conclusion, the proposed oscillator model offers a novel approach to driving biochemical oscillations by exploiting membrane localization and tunability of the V/A ratio. This model has the potential to impact a wide range of applications in synthetic biology, including biosensors and drug delivery. Further

investigation and experimental validation are necessary to fully understand the model's potential and limitations and to pave the way for its application in various contexts.

REFERENCES

1. Elowitz, M.B. and S. Leibler, *A synthetic oscillatory network of transcriptional regulators.* Nature, 2000. **403**(6767): p. 335-338.
2. Olson, E.J. and J.J. Tabor, *Post-translational tools expand the scope of synthetic biology.* Curr Opin Chem Biol, 2012. **16**(3-4): p. 300-6.
3. Gao, X.J., et al., *Programmable protein circuits in living cells.* Science, 2018. **361**(6408): p. 1252-1258.
4. Kimchi, O., et al., *Self-assembly–based posttranslational protein oscillators.* Science Advances, 2020. **6**(51): p. eabc1939.
5. Xiong, D., et al., *Frequency and amplitude control of cortical oscillations by phosphoinositide waves.* Nature Chemical Biology, 2016. **12**(3): p. 159-166.
6. Di Paolo, G. and P. De Camilli, *Phosphoinositides in cell regulation and membrane dynamics.* Nature, 2006. **443**(7112): p. 651-657.
7. Bairstow, S.F., et al., *Type Iγ661 Phosphatidylinositol Phosphate Kinase Directly Interacts with AP2 and Regulates Endocytosis.* Journal of Biological Chemistry, 2006. **281**(29): p. 20632-20642.
8. Haucke, V., *Phosphoinositide regulation of clathrin-mediated endocytosis.* Biochem Soc Trans, 2005. **33**(Pt 6): p. 1285-9.
9. Yogurtcu, O.N. and M.E. Johnson, *Cytosolic proteins can exploit membrane localization to trigger functional assembly.* PLOS Computational Biology, 2018. **14**(3): p. e1006031.